INVESTIGATION OF NLRP13-DRIVEN INNATE IMMUNE RESPONSES

by

Açelya Yılmazer

B.S., Molecular Biology and Genetics, Boğaziçi University, 2015

Submitted to the Institute for Graduate Studies in
Science and Engineering in partial fulfillment of
the requirements for the degree of
Master of Science

Graduate Program in Molecular Biology and Genetics
Boğaziçi University

2018

ACKNOWLEDGEMENTS

Firstly, I would like to thank my supervisor Prof. Nesrin Özören for giving me the opportunity to work in her laboratory and for her guidance. She always supported me to follow my curiosity throughout my master project and allowed me to develop my scientific perspective by giving me freedom to ask new questions about my project and find explanation. I am also thankful to my thesis committee members Assoc. Prof. Ceren Çıracı and Assoc. Prof. Umut Şahin for spending their valuable time to evaluate my thesis.

I am thankful to Yetiş Gültekin and Mustafa Yalçınkaya. Their master thesis projects which were related with NLRP13 constituted important steps to clarify the NLRP13 story. Fortunately, their works bring us to study the roles of NLRP13 in inflammasome activity and macrophage differentiation comprising my master thesis. During my thesis, I benefited from plasmid constructs prepared by both Yetiş Gültekin and Mustafa Yalçınkaya and homemade anti-NLRP13 antibody generated by Mustafa Yalçınkaya. Mustafa Yalçınkaya also helped me when I began my project so I am thankful for his great mentorship and friendship.

I want to thank specially Aybüke Garipcan for her friendship and mentorship and cooperative work relationship in every situation between us. I also want to thank specially Beren Aylan, Ayşin Akpınar, Mesut Berber, Can Gürkaşlar, Kübra Zırhlıoğlu, İlke Süder, and Ezgi Taşköprü for their friendship and help during my master studies and writing the thesis. They have kept my motivation at high level even in hard times and given me a second family. I want also to thank my former and current labmates Sevda Avcı, Orhun Külekçi, Ozan Küçükkase, Alper Çevirgel, Aybeg Günenç, Elif Eren, Hulusi Onur Kuzucu, Seda Yaşa, Aylin Alkan, Gizem Olay Artık, Ozan Otaş and Özen Kaya for sharing knowledge and assisting.

I am also grateful to Ekin Ece Erkan, Emir Erkol, Elif Eski, İbrahim İhsan Taşkıran, Sezgi Canaslan, Ulduz Sophie Afshar, and Burçin Duan Şahbaz for being my friend and sharing knowledge and equipments with me during my experiments.

I would like to thank Boğaziçi University and TÜBİTAK for their financial support during my master thesis.

Finally, I am grateful to my parents Müyesser and Adnan Yılmazer, my brother Oğul Can, and my grandmother Meliha Cihan for their love and endless support under all circumstances and in every decisions that I have taken. My special thanks go to my dream partner Emre Kırgın whose love and support enabled me to overcome every difficult step I met during my master study.

ABSTRACT

INVESTIGATION OF NLRP13-DRIVEN INNATE IMMUNE RESPONSES

NOD-like receptors are the key players of inflammasome activation. NLRP13 is a primate specific member of the NLR family containing PYRIN domain and its role in inflammation is still unknown. Since there is no published literature about NLRP13, our knowledge is restricted with the studies of former lab members. From these works, we know that NLRP13 weakly interacts with pro-Casp-1 and ASC and forms inflammasome-like structures with ASC-Casp-1 in an overexpression system. LPS and ATP are upstream activators of NLRP13 protein levels. On the other hand, NLRP13 levels are reduced when co-transfected with Casp-8 and Casp-9. In this thesis, we focus to find the roles of NLRP13 in inflammasome activation and macrophage differentiation through examination of upstream activators and downstream elements. Firstly, we showed that high levels of NLRP13 increases secretion of IL-1β and TNF-α, while decreases secretion of IL-10 upon LPS/ATP treatment. Then, we observed that NLRP13 shows a *Pseudomonas aeruginosa*-specific innate immune response. Infection of THP-1 monocytes with *P. aeruginosa* increases expression of NLRP13 significantly. The increasing levels of NLRP13 enhanced expression and secretion of pro-inflammatory cytokines IL-1β, TNF-α and IL-6. The expression of IL-1β was diminished with NLRP13-knock down in THP-1 cells. Moreover, protein levels of inflammasome components including pro-IL-β and NLRP3 and maturation of both pro-Casp-1 and pro-Casp-8 were enhanced due to high levels of NLRP13 through activation of NF-κB. NLRP13 positively regulated PMA-differentiation of THP-1 cells by activating AKT and ERK pathways. In addition, we showed that NLPR13 is post-translationally cleaved by Casp-8 through stimulation with LPS/ATP and *P. aeruginosa* that is thought a driving force for the functions of NLRP13 in inflammasome activation and macrophage differentiation.

ÖZET

NLRP13 KAYNAKLI DOĞAL İMMÜN YANITIN İNCELENMESİ

NOD-benzeri alıcılar enflamasyon aktivasyonunda kilit rol oynamaktadırlar. NLR P13 primatlara özgü PYRIN bölgesi içeren bir NLR üyesidir ve enflamasyondaki görevle ri bilinmemektedir. Literatürde NLRP13'le alakalı makale olmadığı için, bilgilerimiz laboratuvarımızın önceki üyelerinin çalışmalarıyla sınırlıydı. Bu çalışmalardan, aşırı ifade edildiklerinde NLRP13'ün pro-Kaspaz-1 ve ASC ile etkileştiği ve ASC-Kaspaz1 ile inflamazom-benzeri yapılar oluşturduğu bilinmekteydi. LPS ve ATP'nin NLRP13 inflamazomunun aktivatörleri olduğu bulunmuştu. Öte yandan, Kaspaz-8 ve Kaspaz-9 ile birlikte transfekte edildiğinde NLRP13'ün seviyesi düşmektedir. Bu tezde, NLRP13'ün enflamasyon aktivasyonu, doğuştan gelen bağışıklık yanıtın düzenlenmesi ve makrofaj farklılaşmasındaki rollerini daha ayrıntılı bir şekilde araştırdık. İlk olarak,insan THP-1 hücrelerine LPS ve ATP muamelesinde, yüksek NLRP13 seviyesinin IL-1β ve TNF-α salımlarını arttırırken, IL-10 salımını düşürdüğünü gösterdik. Daha sonra, NLRP13'ün *Pseudomonos aeruginosa*'ya özgün doğal immün yanıt gösterdiğini gözlemledik. THP-1 monositleri *P. aeruginosa* ile enfekte edildiğinde, NLRP13 protein ifadesi anlamlı bir şekilde artmaktadır. Artan NLRP13 seviyesi, IL-1β, TNF-α ve IL-6 pro-enflamatuvar sitokinlerinin ifadelerini ve salımlarını arttırmaktadır. NLRP13'ün baskılanması IL-1β'nın THP-1 hücrelerindeki ifadesini azaltmaktadır. Dahası, yüksek NLRP13 seviyesi, NF-κB aktivasyonunu sağlayarak, pro-IL-1β ve NLRP3 gibi enflamazom kompleks bileşenlerinin protein seviyelerini ve pro-Kaspaz-1 ve pro-Kaspaz-8'in maturasyonlarını arttırmaktadır. NLRP13 AKT ve ERK'i aktif hale getirerek THP-1 hücrelerinin PMA ile farklılaşmalarını pozitif şekilde düzenlemektedir. Ayrıca, LPS/ATP ya da *P. aeruginosa* ile uyarıldığında, NLRP13'ün Kaspaz-8 tarafından kesildiği gösterilmiştir. Kaspaz-8 ile kesiliminin, NLRP13'ün enflamasyon aktivasyonu ve makrofaj farklılaşmasındaki rollerinde etkili olduğunu düşünmekteyiz.

TABLE OF CONTENTS

LIST OF FIGURES

LIST OF TABLES

LIST OF SYMBOLS

^{o}C	Degree Celcius
h	Hour
g	Gram
g	Gravity
kDa	Kilodalton
L	Liter
M	Molar
mg	Miligram
mM	Milimolar
mm	Milimeter
ml	Mililiter
min	Minute
ng	Nanogram
rpm	Revolutions per Minute
sec	Second
V	Volt

α	Alpha
β	Beta
γ	Gamma
κ	Kappa
μg	Microgram
μm	Micrometer
μM	Micromolar
μl	Microliter

LIST OF ACRONYMS/ABBREVIATIONS

2c11	Home-made monoclonal anti-NLRP13 antibody
Ab	Antibody
AD	Acidic Transactivation Domain
ALRs	Absent in melanoma 2 (AIM2)-like receptors
AP	Alkaline Phosphatase
APC	Antigen Presenting Cell
APS	Ammonium Persulfate
ASC	Apoptosis Associated Speck-Like Protein Containing CARD
ATP	Adenosine Triphosphate
BIR	Baculoviral Inhibitory Repeat-like Domain
BSA	Bovine Serum Albumin
CARD	Caspase Activation and Recruitment Domain
CAS9	CRISPR Associated Protein 9
Caspase	Cysteine-Aspartic Protease
cDNA	Complementary DNA
CLR	C-type Lectin Receptor
CRISPRi	Clustered Regularly Interspaced Short Palindromic Repeats Interference
DAMP	Danger Associated Molecular Patterns
DC	Dendritic Cell
dH_2O	Distilled water
ddH_2O	Double-distilled water
DMEM	Dulbecco's Modified Eagle Medium
DMSO	Dimethyl Sulfoxide
DNA	Deoxyribonucleic Acid
EDTA	Ethylenediaminetetraacetic Acid
EGFP	Enhanced Green Florescent Protein
ELISA	Enzyme-Linked Immunosorben Assay

ER	Endoplasmic Reticulum
ERK	Extracellular Signal-Regulated Kinase
FADD	Fas-associated Protein with Death Domain
FBS	Fetal Bovine Serum
FC	Flow Cytometry
GFP	Green Fluorescence Protein
HBS	Hepes Buffer Saline
HEK293	Human Embryonic Kidney Cells
HLA	Human Leukocyte Antigen
IFN	Interferon
IgG	Immunoglobulin G
IκBα	Nuclear factor of kappa light polypeptide gene enhancer in B-cells inhibitor, alpha
IL	Interleukin
LB	Luria Broth
LRR	Leucin Reach Repeat
LPS	Lipopolysaccharide
MAPK	Mitogen-activating protein kinase
MHC	Major Histocompatibility Complex
MOI	Multiplicity of infection
mRNA	Mesenger RNA
NACHT	Present in NAIP, CIITA, HET-E, and TP1
NaCl	Sodium Chloride
NEAA	Non-esential Amino Acid
NF-κB	Nuclear factor kappa B
NK	Natural Killer
NLR	NOD-Like Receptor
NOD	Nucleotide-binding Oligamerization Domain
OD	Optical Density
PAMP	Pathogen Associated Molecular Pattern
PBS	Phosphate Buffer Saline

PBS-T	Phosphate Buffer Saline and Tween 20
PCR	Polymerase Chain Reaction
PFA	Paraformaldehyde
PI3K/AKT	Phosphoinositide 3-kinase/Protein Kinase B
PMA	Phorbol 12-Myristate 13-Acetate
PRR	Pattern Recognition Receptor
PVDF	Polyvinylidene fluoride
PYD	Pyrin Domain
RLR	RIG-I-like Receptor
RNA	Ribonucleic Acid
ROS	Reactive Oxygen Species
RT	Room Temperature
RT-PCR	Reverse Trascriptase PCR
qPCR	Quantitative PCR
SDS	Sodium Dodecyl Sulfate
SDS-PAGE	SDS-Polyacrylamide Gel Electrophoresis
sgRNA	Single Guide RNA
TBS	Tris Buffered Saline
TBST	Tris Buffered Saline and Tween 20
TEMED	N,N,N',N'-Tetramethyl ethylenediamine
TLR	Toll Like Receptor
TNF	Tumor Necrosis Factor
TRP	Trypsin
Tween 20	Polysorbate
v	Volume
w	Weight
WB	Western Blot
WT	Wild Type

1. INTRODUCTION

1.1. Innate Immunity

The defense mechanisms of humans have been evolved as two lines which are namely innate and adaptive immune systems. In order to fight and completely remove pathogens, these two lines of immunity should cooperate. Innate immunity gives rise to the first line of the defense mechanism by attacking quickly and non-specifically, which in turns leads to the recruitment of adaptive immunity agents to the infection site.

For any pathogenic organisms to enter a body, they should firstly overcome the barriers of the innate immune system. These barriers are classified as physical, chemical, and biological. The external surfaces of bodies are physically protected by the skin and the epithelial sheets provide protection of internal surfaces like gastrointestinal, respiratory, and reproductive tracts. The chemical barriers include secretion of digestive enzymes and anti-microbial peptides from mucosal surfaces like oral cavity and naturally acidic environment of some sites such as stomach and vagina. The biologic barriers consist of normal micro-flora and innate immune cells. In the micro-flora of mucosal surfaces, there are commensal non-pathogenic bacteria which compete with the pathogenic ones for nutrition and secrete antimicrobial molecules against them. If the pathogens succeed to escape these barriers, they are encountered by innate immune cells like macrophages, neutrophils, monocytes, mast cells, and dendritic cells. These cells are recruited the infection site, then they give rise to quick responses by engulfing and destroying the pathogens.

1.2. Pattern Recognition Receptors

The cells of the innate immune system mediate the first line of the defense mechanism through sensing the presence of microorganisms, via their pattern recognition

receptors (PRRs), which recognize pathogen-associated molecular patterns (PAMPs). PAMPs are molecular structures or patterns which are conserved among microbial species and crucial for their survival. Lipopolysaccaride (LPS), muramyl dipeptide (MDP), flagellin and nucleic acids like dsRNA, ssRNA or CpG-DNA are examples for the ligands of PRRs. Along with PAMPs, PRRs are also responsible for detection of endogenous molecules which are released by damaged or infected cells. Such molecules like extracellular ATP or self DNA are called danger-associated molecular patterns (DAMPs). There are four classes of PRR families which have been currently identified. They are Toll-like receptors (TLRs), C-type lectin receptors (CLRs), Retinoic acid-inducible gene (RIG)-I-like receptors (RLRs) and NOD-like receptors (NLRs) [1].

1.2.1. Toll-like Receptors

The TLR family is the firstly identified member of PRRs. They are evolutionarily conserved from the worm Caenorhabditis elegans to mammals. They are type I transmembrane-spanning proteins characterized by extracellular N-terminal leucine-rich repeats (LRRs) and a transmembrane region followed by a cytoplasmic TIR domain, which is homologous to the cytoplasmic domain of IL-1 receptor family members. In mammals, there are thirteen identified members of the TLR family which are responsible for recognizing different structures of invading pathogens outside of the cell or inside of the endosomes or lysosomes. For instance, TLR4 senses lipopolysaccharide, while TLR5 senses flagellin. In addition, endosomal members of TLRs, TLR3, TLR7, and TLR9, are accountable for sensing dsRNA, ssRNA, and CpG-DNA, respectively. [2]

The engagement of toll-specific pathogen associated molecular patterns with extracellular domain of TLRs triggers dimerization of TLRs and some post-translational modifications to recruit TIR-domain-containing adaptor proteins such as MyD88, TRIF, TICAM, and TRAM. These adaptor proteins are responsible for transmission of the signal inside the cell and activation of MyD88- and TRIF-dependent signaling pathways, which in turns leads to the expression of proinflammatory cytokines and type-I interferons, respectively [3].

1.2.2. C-type Lectin Receptors

C-type lectin receptors are a large family of transmembrane and soluble sensors, mainly expressed in myeloid cells and characterized by the presence of carbohydrate-recognition domain. They act as antigen-uptake receptors via their carbohydrate-recognition domain leading to antigen presentation and T-cell polarization. In addition, they are involved in certain signaling cascades which directly activate the expression of proinflammatory molecules or modulate the activity of TLRs. Aside from sensing pathogen derived ligands to initiate immune responses, they are responsible for recognizing endogenous ligands such as self-carbohydrates, proteins and lipids to maintenance homeostasis. For example, the macrophage C-type lectin MINCLE is involved both in sensing fungi infection via recognizing α-mannose and in the detection of spliceosome-associated protein 130 released from necrotic host cells. [4]

1.2.3. RIG-I-like Receptors

RIG-I-like receptors are known as cytoplasmic RNA sensors and mainly function in the detection of viral infections. The RLR family consists of three members: Retinoic acid-inducible gene-I (RIG-I), melanoma differentiation-associated 5 (MDA5), and laboratory of genetics and physiology 2 (LGP2). These three proteins are composed of a central DEAD box helicase/ATPase domain and C-terminal regulatory domain which mediates binding of RNA ligands. In addition, RIG-I and MDA5 share a N-terminal tandem caspase recruitment domain. They are ubiquitously expressed at low levels, while their expression is induced upon viral infection. Consequently, they initiate antiviral responses by producing type I and type III interferons. [5]

1.2.4. NOD-like Receptors

The NLR family is composed of 22 cytoplasmic sensors which are characterized by an N-terminal protein interaction domain, a central NACHT/NOD domain, and a leucine rich repeat (LRR) domain at the C-terminus. NLRs are classified into four

sub-families according to their N-terminal effector domains: the acidic transactivation domain (AD), the baculoviral inhibitory repeat-like domain (BIR), the caspase activation and recruitment domain (CARD), and the pyrin domain (PYD) (Figure 1.1). These effector domains are responsible for signal transduction and inflammatory responses via interacting with other proteins. The central NACHT domain conducts dNTPase activity and oligomerization, while the LRR domain is important for ligand binding. [6]

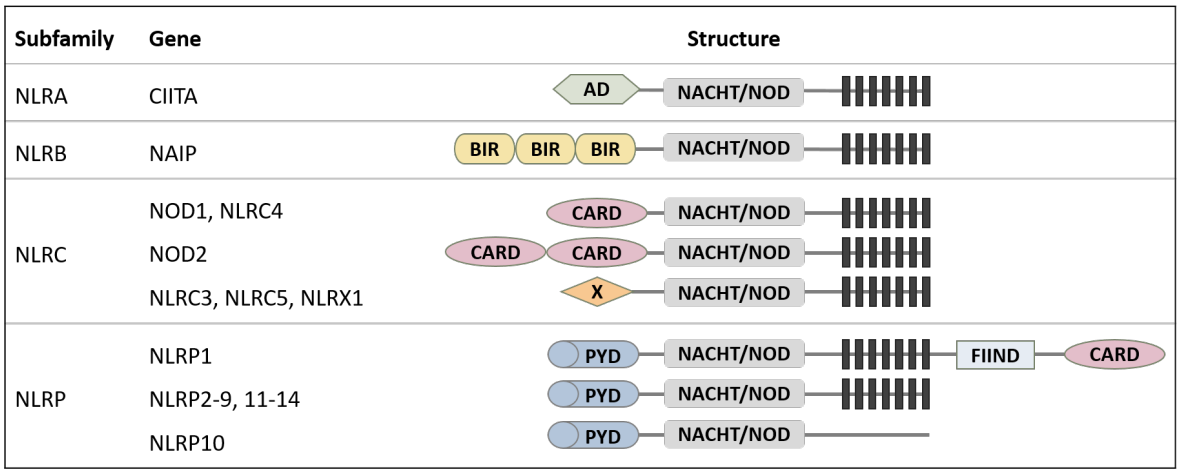

Figure 1.1. NLRs are divided into four subgroups according to their N-terminal effector domains.

NLRs mainly function in inflammasome assembly, signal transduction especially NF-κB signaling, and cell death. Through forming inflammasomes, they induce inflammation and regulate pyroptosis. NLRP1, NLRP2, NLRP3, NLRP6, NLRP7, NLRP12, NLRC4, and NAIP have been shown to be involved in inflammasomes leading to the secretion of inflammatory cytokines upon stimulation by their specific ligands. Along with inflammasome assembly, some NLRs play roles in inflammatory responses via activating or negatively regulating NF-κB and MAPK signaling pathways. For example, upon recognition of cytosolic peptidoglycan ligands, NOD1 and NOD2 oligomerize through their NACHT/NOD domain that allows CARD-CARD interaction with RIP-2 which is serine-therionine kinase that activates NF-κB [7]. In addition to sensing

pathogens and inflammasome activity, NLRs are also key regulators in reproduction, early implantation at fetal-mother interface and embryogenesis. For example, NLRP7 is the first maternal effect gene identified in humans and its mutations cause hydatidiform mole which is an abnormal human pregnancy resulting in miscarriage [8].

1.3. Inflammasomes

Inflammasomes are supramolecular protein complexes which are formed by host defense mechanisms against invading pathogens. Assembly of the inflammasome complex is initiated by nucleotide binding domain and leucine-rich repeat receptors (NLRs) or absent in melanoma 2-like receptors (ALRs). These receptors mediate cytosolic sensing of PAMPs released during infections or DAMPs released from damaged cells that leads to activation of pro-Casp-1.

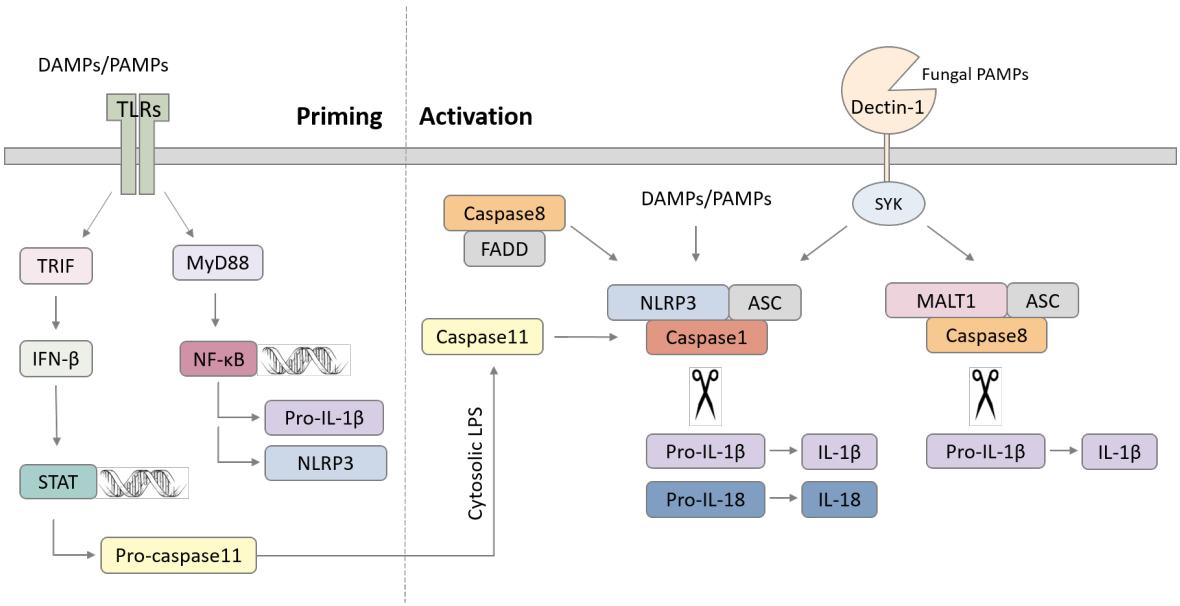

Figure 1.2. Activation of canonical and non-canonical inflammasomes

In most cases, activated NLRs and ALRs recruit an adaptor protein known as apoptosis-associated speck-like protein containing a caspase activation and recruitment domain (ASC). Pyrin domain of ASC interacts with NLRs and ALRs, while ASC is

nucleated into filaments via PYD-PYD and CARD-CARD interactions which further compact in a higher organization level called as speck [9]. Reorganization of cytoplasmic ASC into a speck contributes to recruitment of pro-Casp-1 through CARD-CARD interaction. After assembly of inflammasome complex, maturation of pro-Casp-1 into enzymatically active protease manages the cleavage of pro-inflammatory cytokines such as pro-IL-1β and pro-IL-18 that in turns leads to secretion of cytokines and pyroptosis. [10]

Casp-1 is a crucial player in inflammasome function since outcomes of inflammasome assembly are provided by its enzymatic activity. Apart from Casp-1, recent studies indicate Casp-8, Casp-11, IL-1R-associated kinases (IRAK), and receptor-interacting protein (RIP) kinases contribute to inflammasome function. The inflammasomes, activated by other proteases and kinases rather than Casp-1, are termed as non-canonical inflammasomes. In regard to involvement of proteases and kinases, post-translational modifications like cleavage and phosphorylation are essential for inflammasome activity. [11]

In addition to the functions in host defense against pathogens, inflammasomes are formed during physiological malfunctions. Thus, they play roles in the development of cancer, autoinflammatory, metabolic, and neurodegenerative diseases. For instance, in patients with type 2 diabetes mellitus, circulating monocytes defectively produce IL-1β resulted from impaired NLRP3-inflammasome activity [12].

1.3.1. Canonical Inflammasomes

Inflammasomes consisting of NLRs, adaptor ASC, and Casp-1 are described as canonical. Up to the present; NLRP1, NLRP3, NLRC4, and AIM-2 inflammasomes have been well characterized. AIM-2 is a ALR protein which detects dsDNA from intracellular pathogens like *Mycobacterium tuberculosis* and vaccinia virus via its DNA-binding HIN200 domain [13]. Upon sensing dsDNA, AIM-2 recruit the ASC adaptor protein to activate Casp-1.

Among NLRs, NLRP1 is first identified one forming inflammasomes. NLRP1 is responsible for sensing MDP and anthrax toxin. In response to *Bacillus anthracis* lethal toxin, mouse NLRP1b which lacks pyrin domain at the N-terminus directly recruits pro-casp-1 through CARD-CARD interaction. Lethal toxin cleaves NLRP1b close to its N terminus leading to pyroptosis and IL-1β secretion [14].

Similar to NLRP1b, NLRC4 directly interacts with pro-casp1 through a CARD-CARD interaction. NRLC4-inflammasome is important for host defense against intracellular bacteria like *Salmonella typhimurium* and *Pseudomonas aeruginosa* because NLRC4 senses flagellin and proteins from type III and IV bacterial secretion systems [15]. Like cleavage of NLRP1b, postranslational phosphorylation of NLRC4 at Ser533 improves inflammasome activity upon infection with *S. typhimurium* [16].

The NLRP3-inflammasome is the most studied one. A wide range of DAMPs and PAMPs activating the NLRP3-inflammasome has been characterized. These include danger signals such ATP and ROS, crystalline substances like uric acid, microbial toxins like nigericin. For NLRP3-inflammasome activation, two signals are required. The first signal known as priming step activates the NF-κB pathway through TLRs, NOD2, and TNFR which in turns leads to expression of pro-IL-1β and NLRP3 [17]. The second signal known as activator leads to the assembly of the inflammasome complex. After formation of the complex, activation of Casp-1 results in maturation and secretion of IL-1β. Several mechanisms which work as the activator signal have been proposed. These include potassium efflux, increasing intracellular calcium, translocation of NLRP3 to mitochondria, cytosolic release of lysosomal cathepsins, and cytosolic release of mitochondrial-derived factors such as ROS. For example, extracellular ATP stimulates the purinergic receptor P2X7 which allows passage of small ions including K^+ across the plasma membrane that activates the NLRP3-inflammasome [18]. Furthermore, post-translational modifications are important for activation of NLRP3-inflammasome; removal of ubiquitin chains from the LRR domain of NLRP3 by BRCC3 is required for inflammasome assembly [19].

1.3.2. Non-canonical NLRP3-Inflammasome

Non-canonical inflammasomes are platforms formed by human Casp-4,5,8 and mouse Casp-11 (ortholog of human Casp-4,5) to induce secretion of proinflammatory cytokines and cause pyroptosis. A non-canonical NLRP3-inflammasome formed by Casp-11 is responsible for defense against intracellular Gram-negative bacteria because activation of Casp-11 is stimulated by acylated lipid A, a component of LPS. TLR4-TRIF-mediated recognition of exogenous LPS engenders upstream regulation of Casp-11 expression by activating type I interferon signaling pathway. However, activation of Casp-11 is independent from TLR4 since Casp-11 directly senses endogenous LPS. LPS-induced Casp-11 activation leads to pyroptosis and IL-1α secretion. [20]

Casp-11 does not directly cleave IL-1β and IL-18, still it indirectly promotes secretion of these cytokines via the canonical NLRP3-inflammasome. LPS-induced Casp-11 activation triggers cleavage of the pannexin-1 channel. Activated pannexin-1 channel boosts K+ efflux and extracellular ATP leading to activation of the canonical NLRP3-inflammasome. [21]

Apart from Casp-11, a non-canonical Casp-8 inflammasome has been recently proposed. Evidently, in response to infections with fungi and mycobacteria, the Syk signaling pathway is activated through the dectin-1 receptor. As a consequence, CARD9-BCL10-MALT1 complex promotes activation of NF-κB inducing pro-IL-1β expression. Moreover, inflammasome complex consisting of pro-Casp-8, ASC, and CARD9-BCL10-MALT1 complex assembles leading to the maturation of pro-Casp-8. Then, active Casp-8 cleaves pro-IL-1β. [22]

In addition to forming its own inflammasome complex, Casp-8 provides scaffolding function for both canonical and non-canonical NLRP3-inflammasome. Casp8 and its adapter Fas-associated death domain (FADD) are required for efficient TLR4-induced transcriptional upregulation of NLRP3, pro-Casp-11, and pro-IL-1β. Besides, FADD functions as a platform for maturation of pro-Casp-8. They interact with core

components of NLRP-3 inflammasome and active Casp-8 contributes to Casp-1/11 maturation. [23].

1.3.3. Pyroptosis

Pyroptosis is a nonhomeostatic and lytic mode of cell death which is mediated by activity of inflammatory caspases. Pyroptosis has common features with both apoptosis and necrosis. It is morphologically similar with necrosis because of membrane rapture and cytokine release. Nevertheless, it is a type of programmed and caspase-dependent cell death like apoptosis. Pyroptosis is a key defense against microbial infections. Pyroptotic death of infected cells brings beneficial outcomes for host defense, since it halts replication of intracellular bacteria and promotes elimination of bacteria via exposing them to other circulating innate immune cells.

Gasdermin D (GSDMD) has been recently identified as a caspase substrate and an essential mediator of pyroptosis [24]. In response to infection, Casp-1 and Casp-11 are activated via inflammasomes. Then, they cleave GSDMD generating an N-terminal cleavage product GSDMD-NT which mediates pore formation triggering pyroptosis, releasing IL-1β and many cytosolic DAMPs [25].

1.4. NLRP13

NLRP13, also known as NALP13, NOD14, PAN13, CLR19.7, is located on 19q13.43 in *Homo sapiens*. NLRP13 is a primate specific gene consisting of 12 exons and expected to produce 118kDa protein. There are two splice variants in databases. The variant 1 and 2 comprise 1036 and 1043 amino acids, respectively. They share same amino acid sequence until 1030th amino acid. Like other members of NLR family, NLRP13 contains three functional domain; N-terminal PYD domain, central oligomerization domain NACHT, and C-terminal LRR domain comprising seven leucine rich repeats.

There are only two publications in which NLRP13 has been mentioned. One of them has suggested that *Toxoplasma gondii* infection upregulates the expression of NLRP13 in THP-1 macrophages [26]. The other one related with generation of microfluidic chip to observe drug resistance of cells shows that U87 glioblastoma cells which are resistant to doxorubicin in an *in vitro* tumor microfluidic ecology has a missense mutation in NLRP13 gene [27].

Knowledge from these publications is quite limited and does not allow to understand the role of NLRP13 on the activity of inflammasomes. Nevertheless, our knowledge about NLRP13 has been uniquely extended thanks to the master thesis works of our former lab members Yetiş Gültekin and Mustafa Yalçınkaya. Previously, Gültekin showed that NLRP13 mainly localizes in cytoplasm and partially in mitochondria (%35) and NLRP13 weakly interacts with Casp-1 and ASC and forms inflammasome-like structures together with ASC-Casp-1 when overexpressed in HEK293FT cells [28]. Then, Yalçınkaya showed that LPS and ATP are the upstream activators of NLRP13 in THP-1 macrophages and NLRP13 is post-translationally cleaved by Casp-8 [29].

1.5. Macrophage Differentiation

Monocytes are a type of leukocytes which are circulating in the bloodstream. They undergo specific differentiation to either macrophages or dentritic cells according to signals that come from the local tissue environment. Caspases, especially Casp-8, function in differentiation of monocytes into macrophages. When caspases are blocked by caspase inhibitors, differentiation of human monocytes into macrophages is arrested, whereas differentiation into dentritic cells is not affected [30]. Furhermore, Casp-8 deleted monocytes are prevented from differentiating into macrophages upon treatment with macrophage colony-stimulating factor (M-CSF) [31].

Macrophage diffentiation could be classified within two separate states depending on the microenvironment signals. These includes classically activated/inflammatory(M1) and alternatively activated/regenerative(M2) macrophages. M1 and M2 polarizations

have characteristic profiles of cell surface markers, secreted cytokines, and activated signaling pathways. LPS, IFN-γ, and granulocyte-macrophage colony-stimulating factor (GM-CSF) lead to M1 polarization by regulation of STAT1 and IRF5 transcription factors, while M-CSF, IL-4, IL-13, IL-10, and TGF-beta polarize macrophages towards M2 phenotype through STAT6 and IRF4. M1 macrophages are characterized by secretion of IL-1β, TNF-α, IL-12, IL-18 and IL-23. Thus, they drive cellular response by directing T cells to T_H1 and T_H17 subtypes. They expresses high levels of major histocompatibility complex class II (MHCII), CD68, CD80, and CD86 markers. Unlike M1 macrophages, M2 macrophages secrete high levels of IL-10 and low levels of IL-12 driving T_H2 response. They expresses scavenger mannose and galactose E-type and C-type receptors. [32]

2. PURPOSES

NLRP13 is a novel and uncharacterized member of the NOD-like receptor family containing PYRIN domain. Our lab has previously shown that NLRP13 can interact with pro-caspase-1 and ASC and form inflammasome like structure together with ASC-Casp-1 when overexpressed in HEK293 cells. LPS and ATP were observed as upstream activators for NLRP13 inflammasome and decreasing levels of NLRP13 were detected when co-transfected with Casp-8 or Casp-9. In line with these findings, we aimed to investigate the role of NLRP13 in inflammasome regulation.First, since NLRP13 levels were upregulated by LPS/ATP stimulation, we carried out a cytokine profiling experiment in THP-1 cells stably expressing NLRP13. Second, to identify the pathogens that may trigger the NLRP13-dependent inflammasome activity, we carried out live infection with *Staphylococcus aureus* and *Pseudomnas aeruginosa*. In order to specify cytokine profiling affected by NLRP13 through stimulation with infection, membrane and flow cytometry based cytokine arrays and ELISA were used. Apart from downstream cytokine secretion, the research was focused on investigating the effects of NLRP13 on the protein and mRNA levels of the inflammasome components like Casp-1, Casp-8, ASC, and NLRP3 via WB, FC and q-RT-PCR after infection. For further examination of the roles of NLRP13 in inflammasome activation, NLRP13 knock-down THP-1 human monocytic cells were generated via CRISPR-Cas9 system. At last but not least, the contribution of NLRP13 in M1/M2 macrophage differentiation and in activation of the NF-κB, ERK, and AKT pathways and post-translational cleavage of NLRP13 were studied.

3. MATERIALS

3.1. Cell Lines

3.1.1. THP1 Monocytic Cell Line

The THP1 human monocytic cell line derived from acute monocytic leukemia was kindly provided by Prof. Ahmet Gül from the Istanbul University, (Istanbul, Turkey) and grown in RPMI-1640 supplemented with 10% FBS, 1x MEM Non-Essential Aminoacids, 100 U/ml penicillin and 100 μg/ml streptomycin.

3.1.2. Human Embryonic Kidney Cell Line (HEK293FT)

The HEK293FT cell line was kindly provided by Prof. Maria Soengas from the Spanish National Cancer Research Center (CNIO, Madrid, Spain) and grown in DMEM supplemented with 10% FBS, 1x MEM Non-Essential Aminoacids, 100 U/ml penicillin and 100 μg/ml streptomycin.

3.1.3. HEC1A Endometrial Cancer Cell Line

The HEC1A cell line was purchased from the American Type Culture Collection, Virginia, USA and grown in McCoy's 5A modified media supplemented with 10% FBS, 1x MEM Non-Essential Aminoacids, 100 U/ml penicillin and 100 μg/ml streptomycin.

3.2. Chemicals, Plastic and Glassware

Chemicals were purchased from either Sigma (USA), Applichem (Germany) or Merck (Germany). Plastics from TPP (Switzerland), Axygen (USA), or VWR (USA) were used. Glassware, tips and tubes were sterilized by autoclaving at 121°C for 20 minutes before using.

3.3. Buffers and Solutions

3.3.1. Molecular cloning

Table 3.1: Enzymes used in cloning.

Enzymes/Buffers	**Supplier**
BsmBI FD	Fermantes, USA
FastAP	Fermantes, USA
FastDigest Buffer	Fermantes, USA
T4 DNA Ligase	NEB, USA
T4 DNA Ligase buffer	NEB, USA
T4 PNK	NEB, USA

3.3.2. Cell Culture

Table 3.2: Cell Culture Chemicals.

Chemicals	**Supplier/ Recipe**
ATP	Sigma, USA
DMSO	AppliChem, Germany
Dulbecco's Modified Eagled Medium (DMEM)	Gibco Invitrogen, USA
Fetal Bovine Serum	Gibco Invitrogen, USA
Gentamicin	Sigma, USA
LPS	Sigma, USA
McCoy's 5A (modified) Medium	Gibco Invitrogen, USA

Table 3.2. Cell Culture Chemicals (cont.).

MEM Non-essential amino acid 100X	Gibco Invitrogen, USA
Penicillin/Streptomycin	Gibco Invitrogen, USA
PBS 10X	80 gr NaCl 2gr KCl 2.4 gr KH_2PO_4 14.4 gr Na_2HPO_4 Add ddH_2O up to 1 lt (pH:7.2)
PMA	Sigma, USA
Puromycine	Sigma, USA
RPMI Media 1640	Gibco Invitrogen, USA
0.05% TRP with EDTA	0.154 gr EDTA 0.5 gr Trypsin 8 gr NaCl 0.4 gr KCl 0.06 gr KH_2PO_4 1gr Glucose 0.048 gr Na_2HCO_3 Add ddH_2O up to 1 lt Adjust pH to 8 Filter sterilize
z-VAD-FMK	Promega, USA

3.3.3. Transfection and Transduction

Table 3.3: Transfection and Transduction Reagents.

Reagents	**Supplier/ Recipe**
$CaCl_2$	Merck, USA
2X HBS Buffer	50 mM HEPES pH 7.0 280 mM NaCl 1.5 mM Na_2HPO_4
HEPES	Gibco Invitrogen, USA
Polybren	Sigma, USA

3.3.4. Western Blotting

Table 3.4: Chemicals used in WB.

Solutions/Chemicals	**Recipe/Supplier**
Acrylamide: Bisacrylamide	30 gr Acrylamide 0.8 gr Bisacrylamide in 100 ml ddH_2O
Ammonium Persulfate	10 % APS (w/v)
Blocking Solution	5 % Non-fat milk in TBS-T
Bovine Serum Albumin Fraction V	Roche, Germany
Cell Lysis Buffer	0.2 % NP-40 142 mM KCl 5 mM MgCl2 10 mM Hepes 1 mM EDTA
6X Laemmli Sample Buffer	1.2 gr SDS

Table 3.4. Chemicals used in WB (cont.).

	6 mg Bromophenol Blue 4.7 ml Glycerol 1.2 ml 0.5 M Tris pH 6.8 500 μl β-mercaptoethanol Add ddH_2O up to 10 ml
Methanol	Merck, USA
2-Propanol	Merck, USA
Protease Inhbitor Cocktail	Roche, Germany
Protein Ladder (PI-26617)	Pierce, USA
PVDF membrane	Merck, USA
10 % Resolving Gel	333 ml Acrylamide: Bisacrylamide 10 ml 10 % SDS 200 ml 1.875 M Tris pH 8.8 Add ddH_2O up to 1 lt
15 % Resolving Gel	500 ml Acrylamide: Bisacrylamide 10 ml 10 % SDS 200 ml 1.875 M Tris pH 8.8 Add ddH_2O up to 1 lt
Running Buffer	1X Tris-Glycine Buffer 0.1 % SDS
SDS	AppliChem, Germany
4 % Stacking Gel	3.3 ml Acrylamide: Bisacrylamide 6.3 ml 0.5 M Tris-HCl pH 6.8 250 μl 10 % SDS Add ddH_2O up to 25 ml
10X TBS	90 gr NaCl 121.14 gr Tris-Base Add ddH_2O up to 1 lt pH:7.5
TBS-T	1X TBS 0.1 % Tween-20

Table 3.4. Chemicals used in WB (cont.).

TEMED	Merck, USA
Transfer Buffer	39 mM Glycine 48 mM Tris-Base 0.0625 % SDS pH:9.2
10X Tris-Glycine Buffer	15 gr Tris-Base 72 gr Glycine Add ddH_2O up to 500 ml
TWEEN-20	Sigma-Aldrich, USA
WesternBright ECL HRP substrate	Advansta, USA
WesternBright Sirius HRP substrate	Advansta, USA

3.3.5. ELISA

Table 3.5: Solutions used in ELISA.

Solutions	**Recipe**
Reagent Diluent	1% BSA in 1X PBS
Stop Solution	2N H_2SO_4
Subsrate Solution	1:1 mixture of Color Reagent A (H_2O_2) and Color Reagent B (Tetrametylbenzidine)
Wash Buffer	0.05 % Tween-20 in 1X PBS

3.3.6. Culture of Bacteria

Table 3.6: Chemicals used in culture of bacteria.

Chemicals	**Recipe/Supplier**
Ampicillin	AppliChem, Germany
Chloramphenicol	Sigma-Aldrich, USA
Kanamycin	Sigma-Aldrich, USA
LB Agar	1 L LB medium 15 g Agar
LB Medium	10 g Tryptone 5 g Yeast Extract 5 g NaCl
20X M9 salts	70 g $Na_2HPO_4 \bullet 7H_2O$ 30 g KH_2PO_4 5 g NaCl 10 g NH4Cl ddH2O up to 500 ml
Modified LB	50 ml 20X M9 salts 10 ml 20% glucose 1X kanamycin 1X chloramphenicol

3.3.7. Protein Purification

Table 3.7: Buffers used in protein purification.

Buffers/Chemicals	**Supplier/ Recipe**
Coomassie Blue Solution	0.1 % Coomassie Brilliant Blue R-250 10 % Acetic Acid 50 % Methanol

Table 3.7. Buffers used in protein purification (cont.).

Destainin Solution	40 % Methanol 10 % Acetic acid
Dough's Solution	167 mM Tris-HCl (pH 6.8) 0.5 % SDS 10 % Sucrose 25 μl/ml β-mercaptoethanol 0.01 % Bromophenol Blue
Elution Buffer	50 mM Tris-HCl 150 mM NaCl 0.1 mM EDTA pH 7.5
IPTG	Roche, Germany

3.4. Fine Chemicals

3.4.1. Plasmids

Table 3.8: Plasmids.

Plasmids	**Provider**
pcDNA3-Flag-NLRP13	AKIL, Bogazici University
pcDNA3-GFP-NLRP13	AKIL, Bogazici University
pcDNA3-HA-NLRP13	AKIL, Bogazici University
pcDNA3-Myc-NLRP13	AKIL, Bogazici University
pcDNA3-procaspase-8	Nunez Lab, University of Michigan
pcDNA3-procaspase-8 MT	Nunez Lab, University of Michigan
pet30a-NLRP13	AKIL, Bogazici University

Table 3.8. Plasmids (cont.).

plex307	GenReg, Bogazici University
plex307-empty	AKIL, Bogazici University
plex307-NLRP13	AKIL, Bogazici University
pCW-Cas9	GenReg, Bogazici University
pLKO5.sgRNA.EFS.GFP	GenReg, Bogazici University

3.4.2. Primers

Table 3.9: Primers for RT-qPCR and Sanger Sequencing.

Primer ID	**Sequence (from 5' to 3')**	**Application**
ASC_F	TGGATGCTCTGTACGGGAAG	RT-qPCR
ASC_R	CCAGGCTGGTGTGAAACTGAA	RT-qPCR
BDCA-2_F	TTGAAAGAACCACACCCCGAAAGT	RT-qPCR
BDCA-2_R	TAGCTTTCTACAACGGTGGATGCC	RT-qPCR
Caspase1_F	TTTCCGCAAGGTTCGATTTTCA	RT-qPCR
Caspase1_R	GGCATCTGCGCTCTACCAT	RT-qPCR
CCR7_F	TGGTGGTGGCTCTCCTTGTC	RT-qPCR
CCR7_R	TGTGGTGTTGTCTCCGATGTAATC	RT-qPCR
CD1c_F	TGGTGACAATGCAGACGCA	RT-qPCR
CD1c_R	GGTTGACAAATGAGAAGATCTGGA	RT-qPCR
CD206_F	ACCTCACAAGTATCCACACCATC	RT-qPCR
CD206_R	CTTTCATCACCACACAATCCTC	RT-qPCR
HPRT_F	GCTATAAATTCTTTGCTGACCTGC	RT-qPCR
HPRT_R	AATTACTTTTATGTCCCCTGTTGACT	RT-qPCR
IL-1β_F	TTACAGTGGCAATGAGGATGAC	RT-qPCR
IL-1β_R	GTCGGAGATTCGTAGCTGGAT	RT-qPCR

Table 3.9. Primers for RT-qPCR and Sanger Sequencing (cont.).

IL-6_F	AATTCGGTACATCCTCGACGG	RT-qPCR
IL-6_R	GGTTGTTTTCTGCCAGTGCC	RT-qPCR
NLRP13_F1	ATCCAAACCAAGAAGAACCAGAG	RT-qPCR
NLRP13_R1	TGGTCTTTAGGCCAACTGATGTT	RT-qPCR
NLRP13_F2	AACTTGAGAGCTGCCGACC	RT-qPCR
NLRP13_R2	TCTCTAGATCTTCCTGGGTTG	RT-qPCR
NLRP13_Seq_F1	AGAAGCAGCAGCAGGGAATA	Sequencing
NLRP13_Seq_F2	GGTTCCCCTGGCTACCTTAC	Sequencing
NLRP13_Seq_F3	CATTCCACAAAGCCACAAGA	Sequencing
NLRP13_Seq_F4	ACGTGCAAATCGGTAACTCC	Sequencing
NLRP13_rev_seq	AGTAGGCGCTGCAGTTCCTC	Sequencing
NLRP3_F	CGTGAGTCCCATTAAGATGGAGT	RT-qPCR
NLRP3_R	CCCGACAGTGGATATAGAACAGA	RT-qPCR
pLKO_U6_SEQ_fw	TTTGCTGTACTTTCTATAGTG	Sequencing
TNF_F	CAGGGACCTCTCTCTAATCA	RT-qPCR
TNF_R	AGCTGCCCCTCAGCTTGA	RT-qPCR

3.4.3. Oligos

Table 3.10: sgRNA Oligos

Guide	**Quality score**	**Guide Sequence (from 5' to 3')**	**On-target locus**
1	91	GTAATCACCTGCCCCAACGGTGG	chr19:+5644367
2	79	GGCCCTGGATCAGTATCAGCTGG	chr19:+56443582
3	86	GGACTTCTGGTCGGCCCCCCAGG	chr19:+56443525
4	92	GCACTTCCCGCGTATCCCCTGGG	chr19:+56443526

Table 3.10. sgRNA Oligos (cont.).

5	70	GTGAGGTCAGATTCATTGTCTGG	chr19:-56443369
6	73	AGAGCTGCAAGATCCAACCCAGG	chr19:+56436348

3.4.4. Antibodies

Table 3.11: Antibodies.

Antibodies	**Host/ Isotype**	**Supplier**	**Purpose**
β ACTIN (D6A8)	Rabbit	Cell Signalling Technologies, USA	WB
ASC	Mouse	Prof. Mosumoto, Japan	WB
AKT (pan) (C67E7)	Rabbit	Cell Signalling Technologies, USA	WB
Caspase-1 (P10) (A19)	Rabbit	Santa Cruz Biotechnology, USA	WB
Caspase-1 (P20) (Bally-1)	Mouse	Adipogen Life Sciences, USA	WB
Caspase-8 (1C12)	Mouse	Cell Signalling Technologies, USA	WB
CD11b/MAC-1 Clone ICRF44	FITC	BD Biosciences, USA	FC
CD163 CloneGHI/61	Alexa647	BD Biosciences, USA	FC
CD80 Clone L307.4	Alexa647	BD Biosciences, USA	FC
FLAG	Rabbit	Cell Signalling Technologies, USA	WB

Table 3.11. Antibodies (cont.).

His	Mouse	Santa Cruz Biotechnology, USA	WB
IκBα	Mouse	Cell Signalling Technologies, USA	WB
IgG, Mouse	HRP	Cell Signalling Technologies, USA	WB
IgG, Rabbit	HRP	Cell Signalling Technologies, USA	WB
IgG1, Mouse κ Isotype Control	FITC	BD Biosciences, USA	FC
IgG1, Mouse κ Isotype Control	Alexa647	BD Biosciences, USA	FC
MALT1	Mouse	Santa Cruz Biotechnology, USA	WB
MyD88	Mouse	Santa Cruz Biotechnology, USA	WB
NLRP13	Rabbit	Abcam, UK	WB
NLRP13 (2c11)	Mouse	Homemade	WB
NLRP3 (Cryo-2)	Mouse	Adipogen Life Sciences, USA	WB
p44/42 (Erk1/2) (137F5)	Rabbit	Cell Signalling Technologies, USA	WB
p-AKT (S473)(D9E) XP	Rabbit	Cell Signalling Technologies, USA	WB
p-IκBα	Rabbit	Cell Signalling Technologies, USA	WB
p-p44/p42 (T202/Y204)	Rabbit	Cell Signalling Technologies, USA	WB
Pro-IL-1β (3A6)	Mouse	Cell Signalling Technologies, USA	WB

3.5. Kits

Table 3.12: Kits.

Kits	**Supplier**
DC Protein Assay Kit	Bio-Rad, USA
Direct-zol RNA Miniprep Kit	Zymoresearch
Human IL-β DuoSet	R&D Systems, USA
Human IL-6 DuoSet	R&D Systems, USA
Human TNF-α DuoSet	R&D Systems, USA
Nucleobond Xtra Plus EF Plasmid Isolation Kit	Macherey Nagel, Germany
Nucleospin Gel and PCR Clean-up Kit	Macherey Nagel, Germany
Nucleospin Plasmid Kit	Macherey Nagel, Germany
SensiFAST cDNA Synthesis Kit	Bioline, UK

3.6. Equipments

Table 3.13: Equipments.

Autoclaves	MAC601, Eyela, Japan ASB260T, Astekk, UK
Centrifuges	Allegra X22-R, Beckman, USA Himac CT4200C, Hitachi Koki, Japan J2-MC Centrifuge, Beckman, USA J2-21 Centrifuge, Beckman, USA
Freezers	2021D, Uğur, Turkey 4250T, Uğur, Turkey
Flow cytometer	BD Accuri C6, USA
Incubator	Hepa ClassII Forma Series, Thermo, USA

Table 3.13. Equipments (cont.).

Heat Block	VWR, USA
Laminar Flow Cabinets	Class II ., Tezsan, Turkey
Micropipettes	Gilson, USA
Microscopes	Zeiss, Acio Observer, Germany Zeiss, Axio Observer Z1, Germany Nikon, Eclipse TS100, Netherlands
Microwave Oven	Arçelik, Turkey
pH Meter	Hanna Instruments, USA
Pipettors	VWR, USA
Plate Reader	VersaMax, Molecular Devices, USA
Power supply	Power Pac Universal, BIO-RAD, USA
SDS-PAGE Electrophoresis System	Mini-Protean 4Cell, BIO-RAD, USA
SDS-PAGE Transfer System	Trans-blot Semi-Dry, USA
Sonicator	SonoPlus, Bandelin, Germany
Spectrophotometer	Nanodrop ND-100 Thermo, USA
Shakers	Polymax 1010, USA Polymax 1040, USA Heildophl, Germany
Vortex	Fisons Whirli Mixer, UK GmcLab, Gilson, USA
Water Bath	GFL, Germany
	Polysum
Water filter	UTES, Turkey
Western Blot Visualization	Syngene GBOX, UK

4. METHODS

4.1. Cell Culture

4.1.1. Maintenance of Cells

HEK293FT, Hec1A, and THP-1 cell lines were grown in DMEM-high glucose media, McCoy's 5A modified media, and RPMI-1640 media respectively. Each type of media was containing 10% FBS, 100U/mL Penicillin, 100μg/mL Streptomycin, and 1% non-essential amino acid solution. Cells were maintained in an incubator at 37°C with 5% CO_2. For subculturing of HEK293FT and Hec1A cell lines, the cells were washed with 1X PBS and detached via incubation with trypsin at 37°C. After detachment of cells, media was added to cells in the equal volumes with trypsin to inactivate it. The cells were suspended and cultured in certain ratios according to cell types and experimental procedures. For subculturing of THP1 cells which are non-adherent, the cells were taken into falcon tubes and centrifuged at 500 g for 2 minutes. The media was aspirated and the pellet was resuspended in fresh media.

For long-term storage of cells, the cells were centrifuged at 500 g for 2 minutes and resuspended with freezing media containing 20% FBS and 10% DMSO. Then, the suspended cells were transferred into cryovials and stored at -150°C.

For thawing cells, the cryovials were taken from -150°C and incubated on 37°C water bath. Then, the cell suspension was taken into falcon tubes quickly and mixed with fresh media. The cells were centrifuged at 500 g for 2 minutes, the supernatant was aspirated and the pellet was suspended with fresh media and cultured on fresh culture dishes.

4.1.2. Transfection of HEK293FT cells

HEK293FT cells were transfected with calcium phosphate method. At the day before transfection, the cells were seeded into 10 cm-plates at 70% confluency. Next day, media was aspirated and replaced with fresh media including 25 μM chloroquine. The cells were incubated at 37°C, while the transfection mixture was prepared. 20 μg plasmid DNA was mixed 61 μl 2M $CaCl_2$ and autoclaved double distilled water up to 500 μl. Then, 2X HBS was added to the transfection mixture and mixed very well until bubbles were observed. The transfection mixture was incubated at room temperature for 5 minutes, then given to the cells dropwise. 6 hours later, the media of transfected cells was replaced with fresh media.

4.1.3. Lentiviral Transduction of human THP-1 and Hec1A Cells

In order to produce lentiviruses, HEK293FT cells were transfected with 10 μg corresponding, 7.5 μg psPAX2 envelope and 5 μg p-VSV-G packaging plasmids. Three days later after transfection, media containing lentiviruses was collected and filtered with 0.45 μm filter. Filtered media was divided into eppendorf tubes as 1 ml aliquottes which were stored at -80°C. For transduction of adherent cells, the cells were seeded on six well plates 1 day prior to transduction. The lentivirus aliquot was diluted with media in 1:1 ratio and 2 μg/ml polybrene was added to the mixture. The media of the cells was replaced with the lentivirus containing media. 8 hours later, media was changed.

4.1.4. Generation of THP-1 Cells with Stable NLRP13 Expression

Empty and NLRP13-containing plex307 lentiviral vectors were transfected into HEK293FT cells with helper plasmids to generate lentiviruses. Three days later, the lentiviruses were harvested and THP1 cells were transduced with them. After transduction, the cells were grown for 2 days and 2μg/ml puromycin was given to the cells. Antibiotic selection was performed every two days until killing all infection negative

cells.

4.1.5. Generation of NLRP13 knock out Hec1A and THP-1 Cell Lines

The cells were firstly transduced with lentiviruses containing pCW-Cas9 and infection positive cells were selected via puromycin treatment. Then, stably Cas9-expressing cells were transduced with lentiviruses containing sgRNA oligos cloned within pLKO-5-sgRNA-EFS-GFP vector. The positive cells were determined via the expression of GFP construct of the plasmid and sorted with SH800S Cell Sorter (Sony). In order to generate of NLRP13 knock-out cells, stably Cas9-and sgRNA-expressing cells were treated with 0.1 μg/ml doxycycline in the dark. The treatment was repeated for several days.

4.1.6. Treatments of PMA-differentiated THP-1 Macrophages.

THP-1 monocytes were differentiated into macrophages via 100 ng/ml PMA treatment for 6 hours as 1.5x 10^6 cells/ 6 well-plate. 6 hour later, media of the cells were changed and the cells were allowed to differentiate for 2 days. Then, the cells were treated with the several substances in certain concentrations given in the Table 4.1.

Table 4.1: Substances used for treatment of THP-1 macrophages.

Substances	**Concentration**
LPS	500 ng/ml
ATP	2 mM
z-VAD-FMK	40 μM

4.1.7. Live Infection of Human THP-1 Cells with Pathogenic Bacteria

Glycerol stocks of *Staphylococcus aureus* and *Pseudomnas aeruginosa* were taken from -80°C and grown in 10 ml fresh LB broth without any antibiotics overnight at 37°C on an orbital shaker. On the next day, bacterial cultures were diluted in 1:50 ratio with LB broth until their optical densities were reached to 1 at 600 nm. Then, bacterial cultures were centrifuged at 5000 rpm for 10 minutes at 4°C and washed with cold PBS twice. After washing steps, bacterial pellets were suspended with RPMI-1640 including 10% FBS and 1% MEM-NEA without any antibiotics in certain volumes which were determined according to the count of THP-1 cells and the multiplicity of infection (MOI). When the optical density at 600 nm equals to 1, the bacterial cultures of *S. aureus* and *P. aeruginosa* has 10^7 and 2x10^8 CFU/ml, respectively. In order to infect 1.5x10^6 THP1 cells, 75x10^6 *S. aureus* (MOI:50) and 15x10^6 *P. aeruginosa* (MOI:10) were given to cells. After incubation with bacteria for 2 hours, media were aspirated and the cells were washed with PBS. Then, fresh RPMI-1640 including 10% FBS,1% non-essential amino acid solution 100U/mL Penicillin, 100μg/mL Streptomycin, and 50ng/ml gentamicin was given to cells. After incubation for 2 hours, the cells were again washed with PBS and fresh media were given. Then, the samples were collected at certain time points.

4.2. Molecular Cloning

4.2.1. Plasmid Preparation for sgRNA Oligo Cloning

pLKO-5-sgRNA-EFS-GFP plasmid was received as a glycerol stock from the laboratory of Dr. Tolga Emre and grown in ampicillin containing LB broth by shaking overnight at 37°C. Next day, plasmid DNA was isolated with Nucleobond Xtra Plus EF Plasmid Isolation Kit (Macherey Nagel) according to the instructions of manufacturer. The plasmid DNA were kept at -20°C for long-term storage.

4.2.2. Restriction Enzyme Digestion of pLKO-5-sgRNA-EFS-GFP Plasmid

For the cloning of sgRNA oligos, pLKO-5-sgRNA-EFS-GFP (Addgene 57822) plasmid was digested with BsmBI FD (Fermantes) restriction enzyme. 2 μg of the plasmid DNA was mixed with BsmBI FD restriction enzyme and FastAP (Fermantes) thermosensitive alkaline phosphatase in FastDigest Buffer (Fermantes). The reaction mix was completed to 60 μl with nuclease free double distilled water and the restriction enzyme digestion was performed by incubating the reaction mix at 37°C for 2 hours. After the restriction enzyme digestion, the reaction mix was incubated at 65°C for 10 minutes to inactivate the enzyme.

4.2.3. Agarose Gel Electrophoresis and Extraction of Digested Plasmid

After the restriction digestion of plasmid, all of the digestion product and undigested plasmid as the negative control were mixed with DNA loading dye and loaded into 1% agarose gel including ethidium bromide in order to determine whether the restriction digestion was successfully done. The electrophoresis was performed at 120 V for 30 minutes and the gel was visualized under UV light via Bio-Rad's Gel Doc. In the case of successful digestion, digested band was cut from the gel on a UV box and extracted from the gel by using Nucleospin Gel and PCR Clean-up Kit (Macherey Nagel). The extracted digested plasmid was stored at -20°C for long-term storage.

4.2.4. Design and preparation of sgRNA Oligos

Optimized CRISPR Design tool of MIT was used to determine target guide sequences. The oligos were determined based on the target side sequence (20 bp) and being flanked on the 3' end by a 3 bp NGG PAM sequence and designed as including the restriction sites of BsmBI at the ends of them. Designed target guide sequences with high quality score (min. 70) were ordered and received from Macrogen oligo synthesis services. The oligos were suspended as 100 μM with certain volume of nuclease free double distilled water. Oligo suspensions were kept at -20°C for long-term storage.

4.2.5. Phosphorylation and Anneailing of sgRNA Oligos

In order to phosphorylate and anneal the sgRNA oligos, 1 μl forward and 1 μl reverse oligos were mixed with 1 μl 10x T4 DNA Ligase buffer (NEB) and 0.5 μl T4 PNK (NEB) and the reaction mixes were completed to 10 μl with nuclease free double distilled water. The reaction mixes were firstly incubated at 37°C for 45 minutes in a thermal cycler for phosphorylation reaction. For annealing, the oligos were then incubated at 95°C for 5 minutes, the temperature was decreased to 25°C with 1°C/min rate, and the oligos were lastly incubated at 25°C for 5 minutes. After phosphorylation and annealing of sgRNA Oligos, the samples were mixed with DNA loading dye and run into 1.5% agarose gel to determine whether annealing was successful. Then, the samples were kept at -20°C.

4.2.6. Ligation of Digested Plasmid and Annealed sgRNA Oligos

For ligation of digested plasmid and annealed sgRNA oligos, 50 ng digested plasmid DNA and 1 μl of annealed oligos which were 1:500 diluted with nuclease free double distilled water were mixed with 1 μl 10x T4 DNA Ligase buffer (NEB) and 0.5 μl T4 DNA Ligase (NEB). The reaction mixes were completed to 5 μl with nuclease free double distilled water. For ligation reaction, the mixtures were incubated at 24°C for 90 minutes in a thermal cycler and the enzyme was heat inactivated with following incubation of 10 minutes at 65 °C. Ligation products were used in the transformation directly.

4.2.7. Transformation of Competent Bacteria with Ligation Products

After ligation of digested plasmid and annealed oligos, total amount of ligation products was transformed into Stbl3 E.coli strain which were previously made competent by $CaCl_2$ method. Firstly, competent cells were received from -80°C and incubated on ice for 10 minutes to allow thawing. After thawing of competent cells, 5 μl of ligation products was added into the competent cells near the flame and the mixtures

were incubated on ice for 20 minutes. Then, the competent cells were heat shocked for 45 seconds at 42°C and incubated again on ice for 5 minutes. In order for recovery of heat shocked competent cells, the cells were mixed with 1 ml of LB broth without any antibiotics and incubated at 37°C for 1 hour on an orbital shaker. After recovery, the mixtures were spinned down and the pellets were resuspended in 100 μl of LB broth and spreaded on ampicillin-containing LB-agar plates. The plates were incubated at 37°C overnight as inverted. Next day, the cloning was verified according to number of bacterial colonies on the plates. Several colonies were obtained for ligation products, while there was no colony on the relegation control which was only including digested plasmid.

4.2.8. Validation of Cloning via Sanger Sequencing

Two colonies from each ligation plates were picked and grown into ampicillin-containing LB broth via incubation at 37°C overnight on an orbital shaker. After overnight incubation, the plasmids were isolated with Nucleospin Plasmid Kit (Macherey Nagel) and sent to Macrogen for Sanger sequencing. For the sequencing, pLKO_U6_SEQ_fw primer was used. According to results of sequencing, the plasmids from positive colonies were isolated with Nucleobond Xtra Plus EF Plasmid Isolation Kit (Macherey Nagel) in order to obtain endotoxin free plasmids for transfection.

4.3. Western Blotting

4.3.1. Preparation of protein lysates from cell culture

The cell culture plates were placed on ice, media were aspirated and the cells were washed with ice-cold PBS twice. After washing steps, ice-cold lysis buffer containing protease inhibitor cocktail was added onto plates (150 μl for 6-well plate) and the adherent cells were scraped with plastic cell scraper. Then, the cell suspensions were taken into 1.5 ml eppendorf tubes and incubated on ice for 30 minutes while vortexing periodically. After lysis step, the samples were centrifuged at 13000 rpm for 20 minutes

at 4°C and the supernatants were transferred into fresh tubes. For long-term storages, protein lysates were kept at -20°C.

4.3.2. Determination of protein concentration

DC Protein Assay Kit (Bio-Rad) was used to determine protein concentration of lysates. 5 μl of dilutions of samples and BSA standards were added into 96 well-plate. 25 μl of Reagent A was added to each well. Then, 200 μl of Reagent B was mixed with each sample using a multichannel micropipette. After incubation at room temperature for 15 minutes, absorbance was read via a microplate reader and concentration of each sample was calculated according to equation which was obtained from standard curve. The total protein amount of samples was equalized by adding certain volumes of lysis buffer and each samples was mixed with 5X Laemmlie buffer.

4.3.3. Preparation of SDS-PAGE gels and electrophoresis

8 ml of resolving gel was mixed with 80 μl of 10% APS and 8 μl of TEMED and poured between spacer and short plates. 200 μl of 100% isopropanol was added to gel cassette to flat the gel surface. After polymerization of resolving gel, isopropanol was discarded and 3 ml mixture of 4% stacking gel with 30 μl 10% APS and 3 μl TEMED was poured to the cassette and the comb was inserted into stacking gel. After polymerization of stacking gel, the gel was put into a vertical electrophoresis tank, the tank was filled with 1X running buffer and the comb was removed. The protein samples were denatured by incubation at 95°C for 10 minutes and loaded into the wells. The samples were run at 70V for 30 minutes. After they passed to resolving gel, they were run at 140V for 1 hour.

4.3.4. Semi-Dry Transfer and Membrane Blocking

Pierce Western Blotting Filter Papers (Thermofisher) and Immobilon-PSQ PVDF Membrane (Millipore) were cut in the equal sizes with the gel. PVDF membrane was

activated within 100% methanol by incubation for 1 minute, excess of methanol was removed by immersing the membrane to double distilled water and the membrane was taken into cold semi-dry transfer buffer. Filter papers were soaked with cold semi-dry transfer buffer and one of them was placed onto transfer apparatus. The activated membrane was placed on the filter paper. Then, the gel was put on the membrane and covered by another soaked filter paper. The top of the transfer apparatus was closed and transfer was performed at 10 V for 50 minutes. After transfer, the membrane was taken into a plastic box and blocked with 5 % non-fat milk in TBS-T. Blocking was performed at room temperature for 2 hours on an orbital shaker. After blocking, the membrane was washed with TBS-T three times for 5 minutes.

4.3.5. Incubations with Primary and Secondary Antibodies

After blocking and washing steps, the membrane was incubated with the primary antibody which was 1:1000 diluted with 5% BSA in TBS-T at 4°C overnight on an orbital shaker. After incubation with primary antibody, the membrane was washed with TBS-T three times for 5 minutes at room temperature. Then, secondary antibody was 1:2000 diluted with 5% non-fat milk in TBS-T and the membrane was shaken with the secondary antibody at room temperature for 2 hours. Then, the membrane was again washed with TBS-T three times for 5 minutes.

4.3.6. Visualization and Analysis of Protein Bands

WesternBright ECL-HRP Substrate (Advansta) was used to visualized the protein bands. The substrate was prepared by mixing two solutions in 1:1 ratio, then the membrane was incubated with the substrate for 1 minutes at dark. Visualization of the membrane was performed in SynGene imaging device. For analyses of Western Blotting, the intensity of protein bands was calculated by Image J.

4.4. ELISA for IL-1β, TNF-α, IL-6, and IL-10

4.4.1. Plate Preparation

96-well ELISA microplates were coated with 100 μl capture antibody in working concentration, then the plates were sealed and incubated overnight at room temperature. Next day, each well was aspirated and washed three times with 400 μl wash buffer. To remove wash buffer, the plates were blotted against clean paper towels after each washing steps. After washing, the plates were blocked by adding 300 μl of reagent diluent to each well and incubating at room temperature for minimum 1 hour. After blocking, the plates were washed three times.

4.4.2. ELISA Assay Procedure

Samples were diluted in certain ratios and standards were prepared via dilutions with reagent diluent. 100 μl of samples and standards was added to wells and the plates were incubated at room temperature for 2 hours. Before detection antibody, the plates were washed three times. 100 μl of detection antibody was adding to each well and the plates were incubated at room temperature for 2 hours. Aspiration/washing steps were repeated three times and 100 μl of the working dilution of Streptavidin-HRP was added to each well. After this step, the plates were avoided to be placed in direct light. The plates were incubated with Streptavidin-HRP at room temperature for 20 minutes. Then, last aspiration/washing steps were done and 100 μl of Substrate Solution which is 1:1 mixture of Solution A (H_2O_2) and Solution B (Tetramethylbenzidine) was added to each well. The plates were incubated at room temperature for 20 minutes and 50 μl of Stop solution was added to each well. The plates were gently tapped and optical density of each well were determined immediately with a microplate reader, subtracting the readings at 540 nm from the readings at 450 nm.

4.5. Human Inflammatory Cytokine Arrays

4.5.1. Human Bead Array

THP1 cells stably expressing NLRP13 and control THP1 cells were infected with live *S. aureus* (MOI:50) and *P. aeruginosa* (MOI:10). The supernatants were collected and kept at 4°C. BD Cytometric Bead Array (CBA) Human Inflammatory Cytokines Kit was used to determine secreted cytokines. The Mixed Human Inflammatory Cytokines Capture Beads was vortexed vigorously and 50 μl was added to the appropriate assay tubes. Then, 50 μl of the Human Inflammatory Cytokines Standard dilutions and the samples in certain dilutions was added to the control assay tubes and test assay tubes, respectively. The assay tubes were incubated for 3 hours at room temperature. During this incubation, the Cytometer Setup procedure was performed according to the instructions of manufacturer. After the incubation, 1 ml of Wash Buffer was added to each assay tube and the samples were centrifuged at 200 $\times$ g for 5 minutes. The supernatants were carefully aspirated and discarded and the bead pellets were resuspended with 300 μl of Wash Buffer. Then, the samples were analyzed on BD ACCURI C6 Plus Flow Cytometer. Each sample was immediately vortexed for 3-5 seconds before analyzing. The analysis of data was accomplished via FCAP Array v3 software.

4.5.2. Membrane-based Human Inflammation Antibody Array

THP1 cells stably expressing NLRP13 and control THP1 cells were infected with live *P. aeruginosa* in MOI:10. The supernatants were collected and kept at 4°C. The secreted cytokines were detected via Abcam Human Inflammation Antibody Array - Membrane (ab134003). The array membranes were incubated with 1X Array blocking buffer for 30 min at room temperature. After blocking of the membranes, 1 ml of serum for each sample was added onto the membrane and the membranes were incubated overnight at 4°C on an orbital shaker. On the next day, the membranes were washed with 1X Array wash buffer I for 5 min three times and with 1X Array wash buffer II for 5 min two times. Then, 1 ml of 1X Biotin-Conjugated Anti-Cytokines

was given to each membrane and the membranes were incubated for 2 hours at room temperature. Then, the membranes were washed again as mentioned above and 2 ml of 1X HRP-Conjugated Streptavidin was given to membranes. After 2h incubation at room temperature, washing steps were repeated. After last washing step, 1:1 mixture of Detection Buffer C and Detection Buffer D was put on the membranes and cytokines were detected by chemiluminescence via CCD cameras of SynGene imaging system. The intensity of each dot was determined via ImageJ and normalized to control dots to obtain comparative cytokine secretions.

4.6. Real Time Quantitative PCR (q-RT-PCR)

4.6.1. RNA Isolation

In order to obtain total RNA, Direct-zol RNA Miniprep Kit (Zymoresearch) was used. Firstly, the media of cells were aspirated, the cells were washed with 1X PBS and lysed with appropriate volumes of Trizol. Then, the lysates were loaded on the columns and following steps were proceeded according to the instructions of manufacturers. Optional DNase treatment was performed to remove DNA contaminants. RNA samples were eluted with nuclease free water and the concentration of them was measured using nanodrop. After RNA isolation, 1 μg of each RNA sample was immediately converted into cDNA by using SensiFAST cDNA Synthesis Kit (BIOLINE) and the rest of the samples were kept at -80°C.

4.6.2. Synthesis of cDNA

For convertion of RNA into cDNA, the samples were mixed with 4 μl 5x TransAmp Buffer and 1 μl Reverse Transcriptase and the mixtures were completed to 20 μl with nuclease-free water. By using a thermal cycler, primers were annealed at 25 °C for 10 min, reverse transcription was performed with incubation at 42 °C for 15 min and following incubation at 48 °C for 15 min, and the enzyme was finally inactivated at 85 °C for 5 min. The cDNAs were stored at -20°C.

4.6.3. q-RT-PCR

In order to determine expression levels of several genes, 2 μl of cDNA was mixed with 5 μl SensiFAST SYBR No-ROX (BIOLINE), 0.25 μl of 10 mM forward primer, 0.25 μl of 10 mM reverse primer, and 2.5 μl nulease-free water within 96-well qPCR plate. PCR reaction was performed in Exicycler 96 (Bioneer) machine. Detected Cq values were used to calculate the relative expression of genes and the expression of each gene was normalized to HPRT house-keeping gene.

4.7. Immunoprecipitation

The cells were scraped on ice without removing media and centrifuged at 300 g for 2 min. Then, the cells were washed twice with cold 1X PBS. After washing, the cells were suspended with 900 μl NP-40 containing protease inhibitor cocktail (PIC) and incubated on ice for 20 min, then vortex was performed gently. After incubation, the sample was centrifuged at 13000, 4°C for 20 min and the supernatant was kept. During centrifugation, the beads were taken from 4°C and vortexed. 150 μl beads were calibrated by washing 3 times with 300 μl NP-40 with PIC and centrifugation at 13000 rpm for 20 sec. Then, 50 μl of the supernatant was separated as whole cell lysate, the rest of the sample was given to the calibrated beads and incubated on shaker at room temperature for 30 minutes. During the incubation of the whole cell lysates with the beads, 180 μl beads for IgG and 180 μl beads for corresponding antibody were washed three times with 400 μl NP-40 with PIC via centrifugation at 13000 rpm for 20 sec. After preclearing, 50 μl of the sample was kept and the rest of the precleared sample was divided into two tubes of the calibrated beads. 10 μg of IgG and the corresponding antibody were added to separate tubes. The tubes were incubated on shaker at 4°C. After overnight incubation, flow through samples were kept by pulling down beads via centrifugation at 6500 rpm for 20 sec. The samples were three times washed with 200 μl NP-40 with PIC, the supernatants were kept after each washing step. Then, 2X Laemmlie buffer was added to the beads and western blotting was performed in order to verify the success of immunoprecipitation and to check possible interactions.

4.8. Cell Surface Staining for flow cytometry

The cells were detached via incubation with cold PBS containing 10 mM EDTA on ice for 30 min and the remaining attached cells were gently scraped. The cells were centrifuged at 300 g for 5 min. The supernatants were carefully aspirated and the cells were washed with Stain buffer (BD) two times. Then, the cells were suspended with 100 μl Stain buffer containing 2 μg of Human Fc Block (BD) and incubated at RT for 10 min. The cells were centrifuged at 300 g for 5 min and resuspended with fluorescent antibodies diluted to their recommended optimal concentrations in Stain Buffer. After incubation with antibodies for 30 min at 4°C, the cells were washed with Stain Buffer two times. Then, the cells were finally resuspended with Stain buffer and analyzed with Sony Sorter SH800S. The analysis of samples was performed using Flow Jo software compared to the isotype and compensation controls.

4.9. NLRP13 Processing with Caspase8

4.9.1. NLRP13 Production via IPTG Induction

Pet30a vector containing NLRP13 coding sequence which was cloned previously by Gültekin was transformed into Rosetta pLysS *E. coli* strain via heat shock technique. The transformed bacteria were spread on LB agar plate containing kanamycin and chloramphenicol. The plate was incubated overnight at 37°C. Next day, a colony was selected and streaked on a second LB agar plate containing kanamycin and chloramphenicol. After overnight incubation at 37°C, a colony was picked and growth overnight in 10 ml modified LB broth. After overnight incubation, bacterial culture was diluted as 1:100 with modified LB broth as final volume would be 1 L. The diluted bacterial culture was incubated at 37°C on an orbital shaker and optical density at 600 nm was measured until it would be 0.8. Then, 10 ml of culture was separated for no IPTG control and IPTG was given to the rest of the culture with 1mM final concentration. The culture was shaken at 18°C for 8 hours. The samples were centrifuged at 5000 rpm for 10 min at 4°C, the supernatants were discarded, and the pellets were

stored at -80°C for purification.

4.9.2. NLRP13 Purification from Gel Slices

Purification of NLRP13 was not achieved using His Bind Quick Purification Cartridges, since NLRP13 is a hydrophobic protein and makes insoluble precipitates as an inclusion body. Therefore, the bacterial pellet was suspended with 1X PBS containing 1% Triton X-100. Then, the bacterial suspension was sonicated 3 seconds 3 cycles with 50% power in 15 ml falcon tubes on ice. The sonication was performed 10 times. Then, sonicated sample was centrifuged at 5000 rpm for 10 min at 4°C and sonication-centrifugation steps were repeated two more times. For each step, samples both from pellets and supernatants were collected. Final pellet was dissolved with 1X PBS. Then, the final sample was mixed with Dough's solution and heated at 95°C for 10 minutes. The sample was run in 10% polyacrylamide gel with one regular well for ladder and one large well for sample. After running of the sample, the gel was cut above 100 kDa and below 130 kDa and excised gel was crushed thoroughly with elution buffer (50 mM Tris-HCl, 150 mM NaCl, 0.1 mM EDTA pH 7.5). The homogenized gel-buffer solution was incubated at 30°C on an orbital shaker overnight. On the next day, the solution was centrifuged at 10000g for 10 minutes and the supernatant was kept at -20°C. The purity and concentration of the sample were determined with Coomassie Blue staining via quantification of several BSA standards with ImageJ. For Coomassie Blue staining, the samples were run in 0.75 mm polyacrylamide gel, the gel was stained with Coomasie Blue for 20 min on an orbital shaker at room temperature and destained with detaining solution for 1 hour.

4.9.3. *In vitro* cleavage assay with Caspase8

0.1 μg purified NLRP13 was cleaved with 1 μl human recombinant Casp-8 in 1h reaction at 37°C with a reaction solution containing 50 mM Hepes, pH 7.2, 50 mM NaCl, 0.1% Chaps, 10 mM EDTA, 5% Glycerol, and 10 mM DTT. Then, western blotting against NLRP13 was performed to check the cleavage.

4.10. Statistical Analysis

Statistical analysis was performed with GraphPad Prism 6.0x software. At graphs, the data were demonstrated as mean ± standard deviation. The comparisons between two groups were done by using Multiple t-test and the ones within a group were done by ANOVA and Bonferroni (as post-hoc). For all of the tests, significance criteria was $p<0.05$. All experiments were repeated independently, at least three times. ns: nonsignificant, *$p<0.05$, **$p<0.01$, ***$p<0.001$, ****$p<0.0001$.

5. RESULTS

5.1. Generation of THP-1 Cells with Stable NLRP13 expression

In order to investigate the effects of NLRP13 overexpression on the secretion of cytokines during inflammation, stably-NLRP13 expressing THP-1 human monocytic cell line was required. Firstly, NLRP13 protein levels in stable cells which were generated by Yalçınkaya were checked via WB with homemade monoclonal anti-NLRP13 ab (2c11) produced by Yalçınkaya (Figure 5.1a). The level of NLRP13 was not as high as we expected.

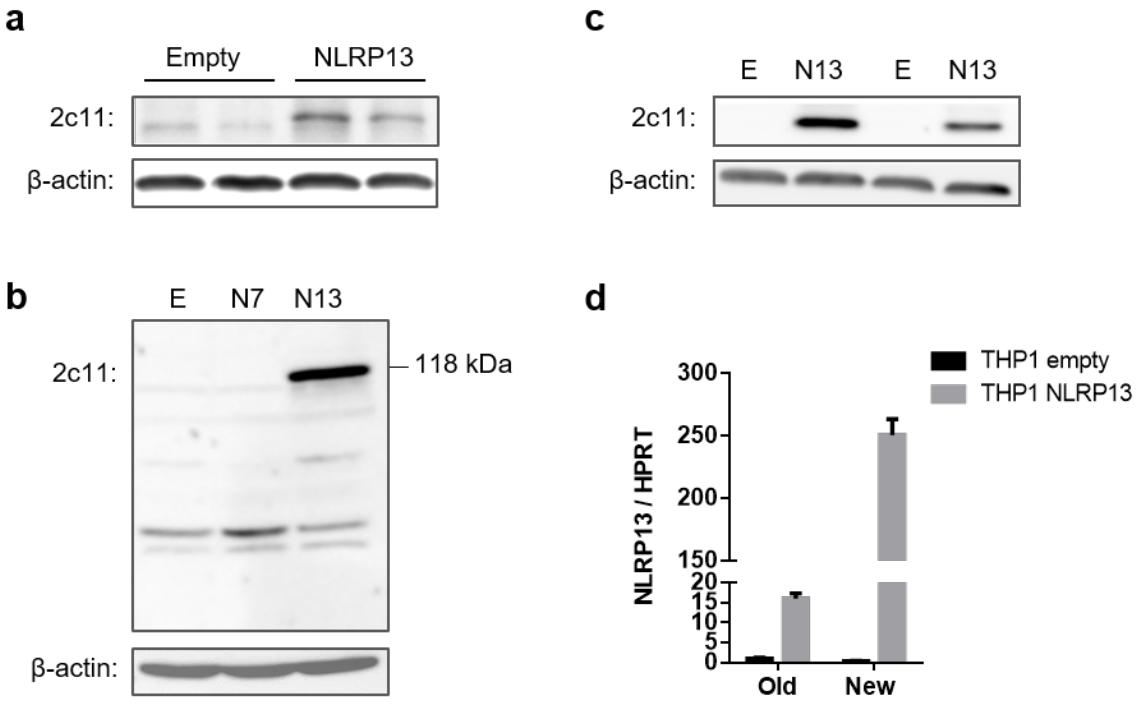

Figure 5.1. Stable NLRP13 expression in THP1 cells. (a,b) NLRP13 expression of previously (a) and recently generated THP1 cells (b) was inspected via WB. (c,d) NLRP13 levels of previously and recently generated stable cells were compared with WB (c) and q-RT-PCR (d). E:empty; N7:NLRP7; N13:NLRP13

We decided to generate new stable cell lines. Thus, plex307-NLRP13 which was previously cloned by Yalçınkaya and plex307-empty vectors were used to produce lentiviruses. After puromycin selection of THP-1 cells transduced with these viruses, we confirmed the stable expression of NLRP13 in THP-1 cells transduced with plex307-NLRP13 containing viruses (Figure 5.1b). Moreover, high protein and RNA levels of NLRP13 in the recently generated THP-1 cells were shown by WB and q-RT-PCR (Figure 5.1c,d).

5.2. NLRP13 Leads to Increasing Secretion of IL-1β and TNF-α and Decreasing Secretion of IL-10 upon LPS and ATP Treatment.

According to the thesis of Yalçınkaya, we know that LPS and ATP are putative upregulators of NLRP13 levels in inflammation. In order to investigate the cytokines downstream of NLRP13, stably-NLRP13 expressing THP-1 cells and control cells were differentiated with 0.5 μM PMA for 3 hours. After 3 h PMA treatment, media of cells were changed. One day later, the cells were primed with 500 ng/ml LPS for 3 h and treated with 2 mM ATP for 30 min. Then, pro-IL-1β protein level was detected with WB and secretion of pro- and anti-inflammatory cytokines was examined via ELISA (Figure 5.2). We observed that NLRP13 increases expression of pro-IL-1β upon LPS and ATP treatment (Figure 5.2b). Consistent with pro-IL-1β, IL-1β secretion was enhanced from 1100 to 1400 pg/ml by NLRP13 overexpression. Besides, high levels of NLRP13 engendered increase in TNF-α secretion from 14 to 21 ng/ml and decrease in IL-10 secretion from 19 to 0.6 pg/ml upon treatment with LPS and ATP. The changes in cytokine secretions were statistically significant.

However, we decided to consider the impact of PMA differentiation in the cytokine secretion profiles. Accordingly, THP-1 cells' differentiation protocol was modified. The cells were treated 100 ng/ml PMA for 9 hours. After 9 h PMA treatment, media of cells were changed. Two days later, the cells were primed with 500 ng/ml LPS for 3 h and treated with 2 mM ATP for 30 min. As divergent from the first experiment, one group of cells were treated with 40μM pan-caspase inhibitor z-VAD-FMK along

with LPS. Consistent with the previous results, the increase in expression of pro-ILβ upon treatment with LPS and ATP was two-fold enhanced with high levels of NLRP13 (Figure 5.3b). The higher NLRP13 expression resulted in the higher secretion levels of IL-1β and TNF-α and the lower secretion level of IL-10. As demonstrated in Figure 5.3c, NLRP13 increased IL-1β secretion from 1200 to 1800 pg/ml and TNF-α secretion from 18 to 44 ng/ml, while it decreased IL-10 secretion from 30 to 4 pg/ml upon LPS/ATP treatment. The difference of cytokine secretions between THP-1 macrophages with stable NLRP13 expression and control cells was two-fold increased with extended PMA-differentiation.

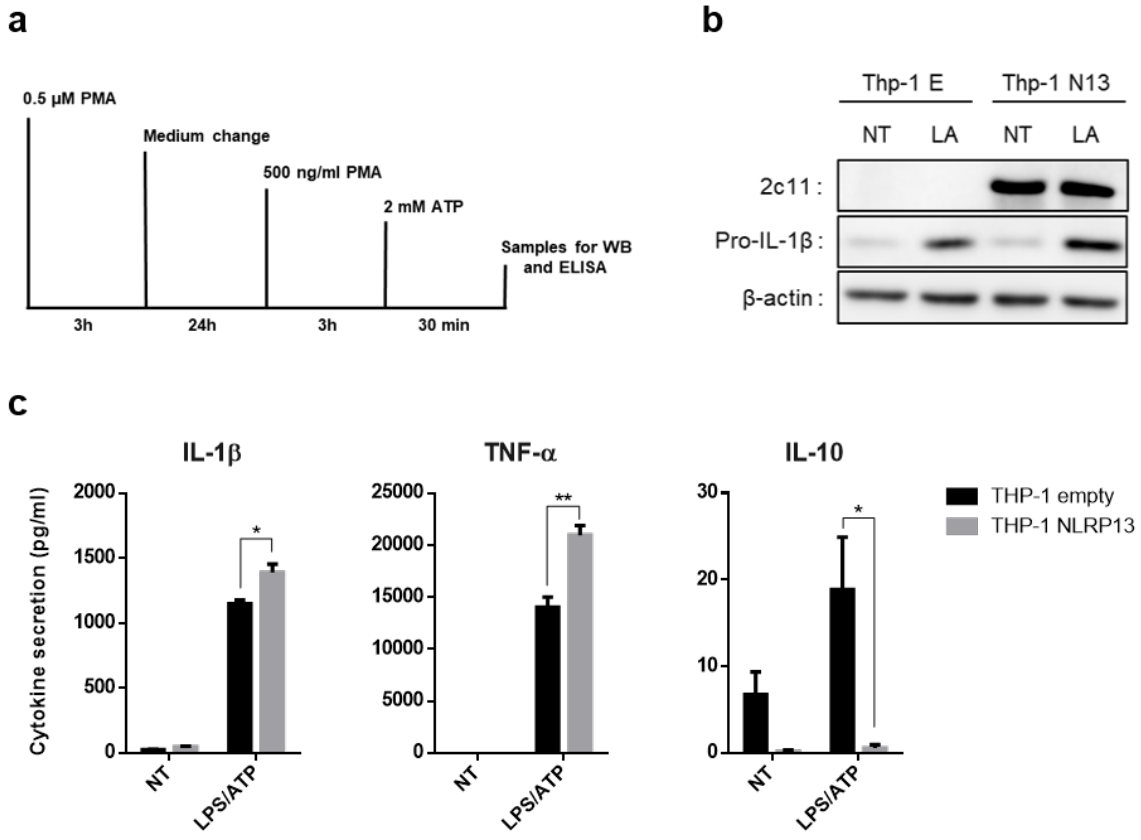

Figure 5.2. High levels of NLRP13 enhance secretion of inflammatory cytokines upon treatment with LPS/ATP. (a) Experimental procedure. (b) NLRP13, pro-IL-1β, and β-actin were detected with WB. (c) Cytokine secretions were measured via ELISA. NT:Nontreated; LA:LPS/ATP. N=6; Multiple t-Test; *p<0.05, **p<0.01; mean ± SD

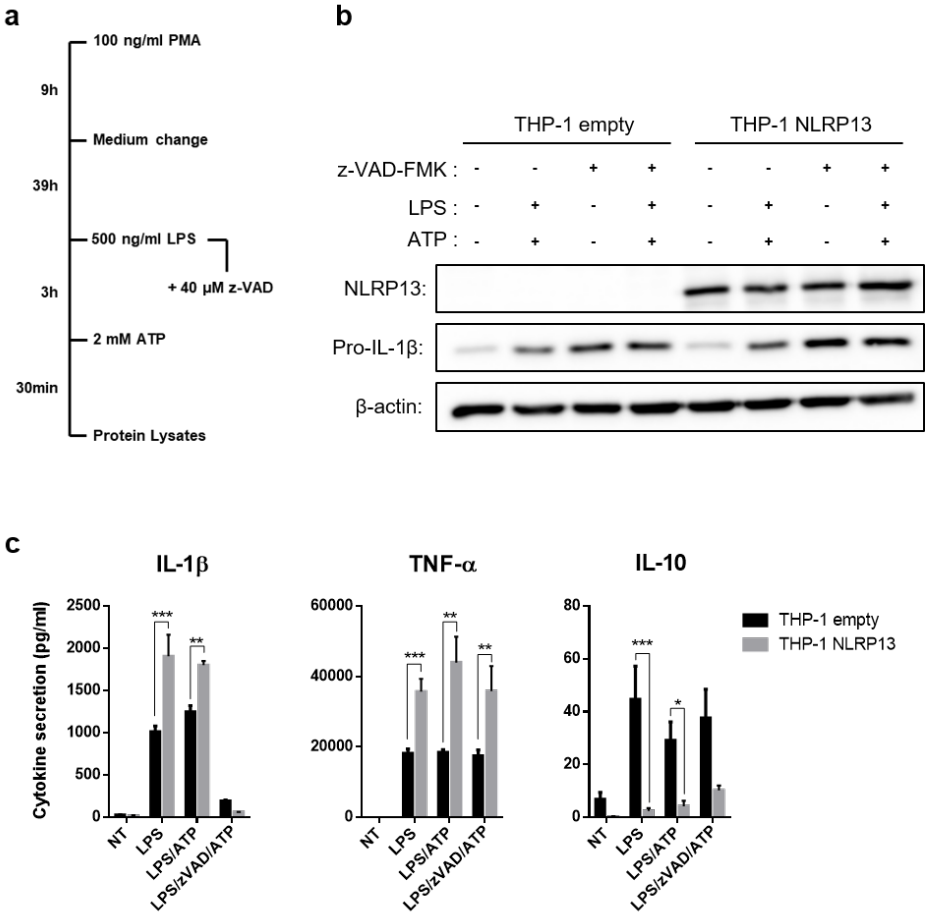

Figure 5.3. Extended PMA differentiation advances the effects of NLRP13 on inflammatory cytokine secretion. (a) Experimental procedure. (b) Results of WB for NLRP13, pro-IL-1β, and β-actin. (c) Cytokine secretions were measured via ELISA. N=3; Multiple t-Test; *p<0.05, **p<0.01;***p<0.001; mean ± SD

The effects of NLRP13 on cytokine secretion upon LPS and ATP treatment were statistically highly significant. When treated with only LPS, the stably-NLRP13 expressing cells secreted more IL-1β and TNF-α and less IL-10 compared to control cells. In addition, z-VAD-FMK treatment led to inhibition of IL-1β secretion, while secretion of TNF-α and IL-10 was not affected. Indeed, NLRP13 contributed to augmentation in secretion of TNF-α upon LPS/z-VAD-FMK/ATP treatment. In this section, the main conclusion would be that there is an additive effect of stable NLRP13 protein expression on LPS/ATP induced cytokine secretions.

5.3. Pathogen-specific Activity of NLRP13

It was shown that higher levels of NLRP13 increases secretion of pro-inflammatory IL-1β and TNF-α and decreases secretion of anti-inflammatory IL-10 upon treatment with LPS or LPS/ATP. In line with these findings, we asked which pathogen may stimulate NLRP13-driven inflammasome activity. Therefore, stably-NLRP13 expressing THP-1 cells and control cells were differentiated with 0.5 μM PMA for 3h. On the next day, the cells were infected with *S.aureus* (MOI:50) and *P.aeruginosa* (MOI:10). The supernatants were collected after 16h infection and samples were analyzed with human cytokine bead array, which is a flow cytometry based array.

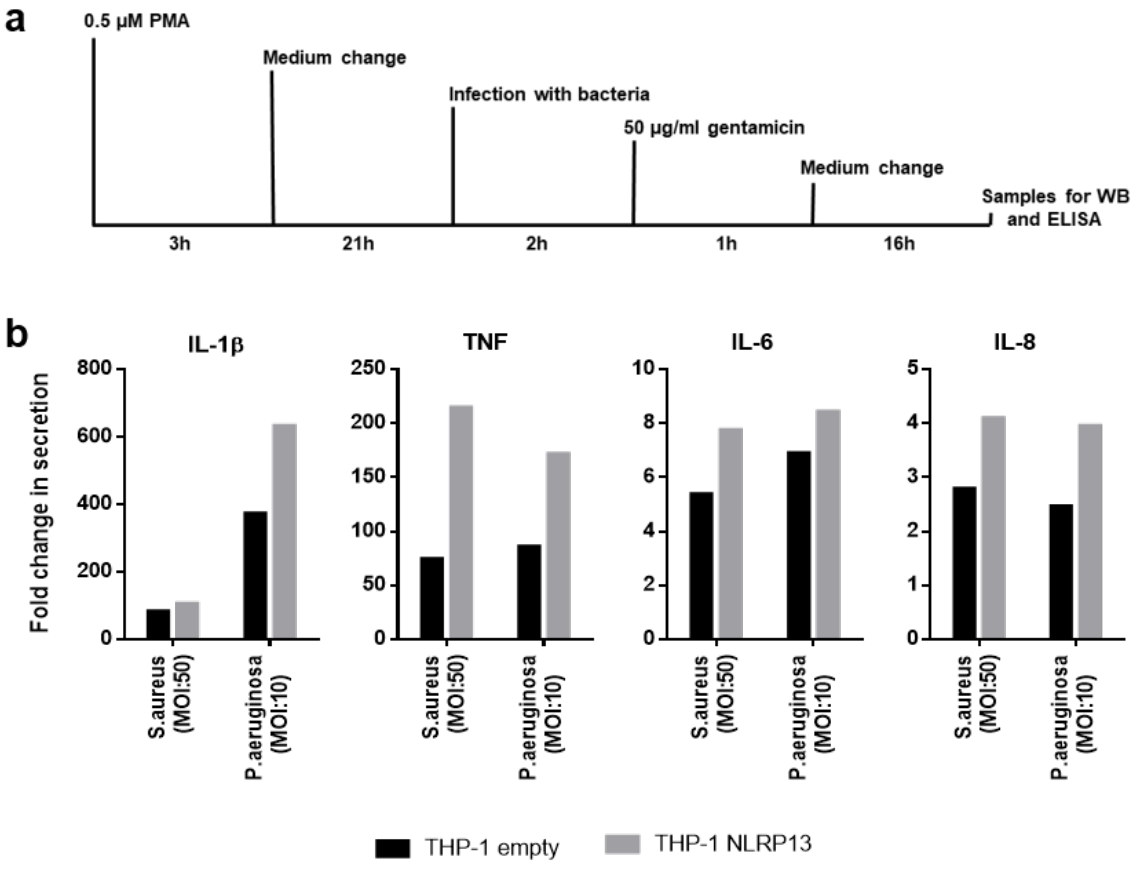

Figure 5.4. (a) Experimental procedure for live infection of PMA-differentiated THP-1 cells. (b) Fold changes of cytokine secretions in infected cells compared to noninfected cells. Cytokine secretions were detected via human inflammatory cytokine bead array.

The bead array was used for screening pathogen-dependent cytokine downstream of NLRP13. The results represent fold changes of secretion levels in infected cells compared to non-infected cells. As seen in Figure 5.4, secretion levels of TNF-α, IL-6, and IL-8 were enhanced with high levels of NLRP13 upon both *S.aureus* and *P.aeruginosa* infection. Interestingly, secretion of IL-1β was two fold increased by high NLRP13 levels upon live infection with *P.aeruginosa*, whereas NLRP13 level did not affect IL-1β secretion in the case of infection with *S.aureus*. The bead array also gives results for the secretions of IL-12 and IL-10; however, in our experiment, these cytokines were not detected.

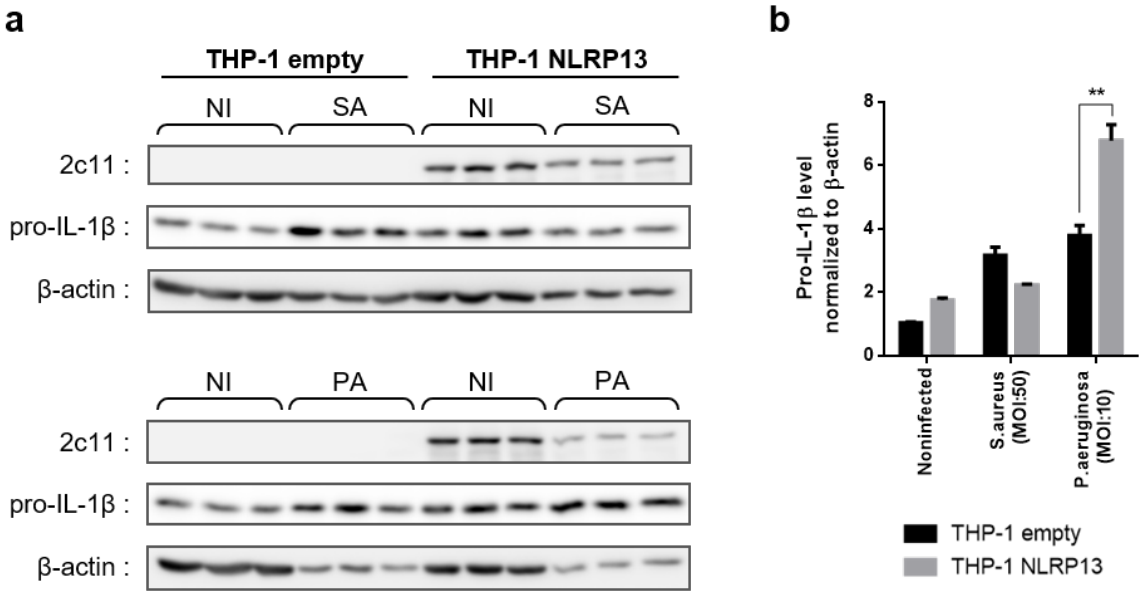

Figure 5.5. NLRP13 overexpression gives rise to pro-inflammatory response against *P.aeruginosa* , but not against *S.aureus*.(a) NLRP13, pro-IL-1β and β-actin were detected with specific antibodies. (b) Quantification of WB results. NI:Noninfected; SA:*S.aureus*; PA:*P.aeruginosa*. N=3; Multiple t-Test; **p<0.01; mean ± SD

Since IL-1β secretion was enhanced by NLRP13 against *P.aeruginosa*, but not against *S.aureus*, the cells were differentiated and infected as described in Figure 5.4a. Then, pro-IL-1β expression was detected via WB (Figure 5.5). When normalized to β-actin used for loading control, it was observed that NLRP13 overexpression contributes

to statistically significant increase in expression of pro-IL-1β upon *P.aeruginosa* infection, while it did not have any influence upon *S.aureus* infection. According to this section, NLRP13 might have additive effects on IL-β processing through immune response to *P.aeruginosa*.

5.4. NLRP13-dependent Innate Immune Response against *P.aeruginosa*

5.4.1. Cytokines Downstream of NLRP13

According to the results shown in Figure 5.4 and 5.5, NLRP13 seems to work in *P.aeruginosa*-specific inflammatory response. In order to investigate the downstream cytokines of NLRP13 upon live infection with *P.aeruginosa*, THP-1 stably expressing NLRP13 and control cells were differentiated with PMA for 3 h. One day later after differentiation, THP-1 macrophages were infected with *P.aeruginosa* (MOI:10). The supernatants were collected after 16h infection. The secreted cytokine profile was analyzed with a membrane-based human cytokine dot blot array (Figure 5.6). Four dots staying upper left corner and two dots staying lower right corner of each membranes are biotin-conjugated IgG printed directly onto the array membrane as positive controls. The normalized densities of each dots within a membrane was calculated by multiplication of densities of each dots with mean signal densities of positive dots in this membrane divided to mean signal densities of positive dots in a reference membrane.

As expected, noninfected PMA-differentiated cells secreted lower levels of cytokines than infected macrophages. Although the secretion levels were low, stably-NLRP13 expressing THP-1 macrophages secreted more IL-1β, IL-8 and MIP-1β compared to control cells (Figure 5.6b). After infection, NLRP13 overexpression contributed to increase in secretion levels of pro-inflammatory cytokines like IL-1β, IL-6, IP-10, and M-CSF (Figure 5.6c).

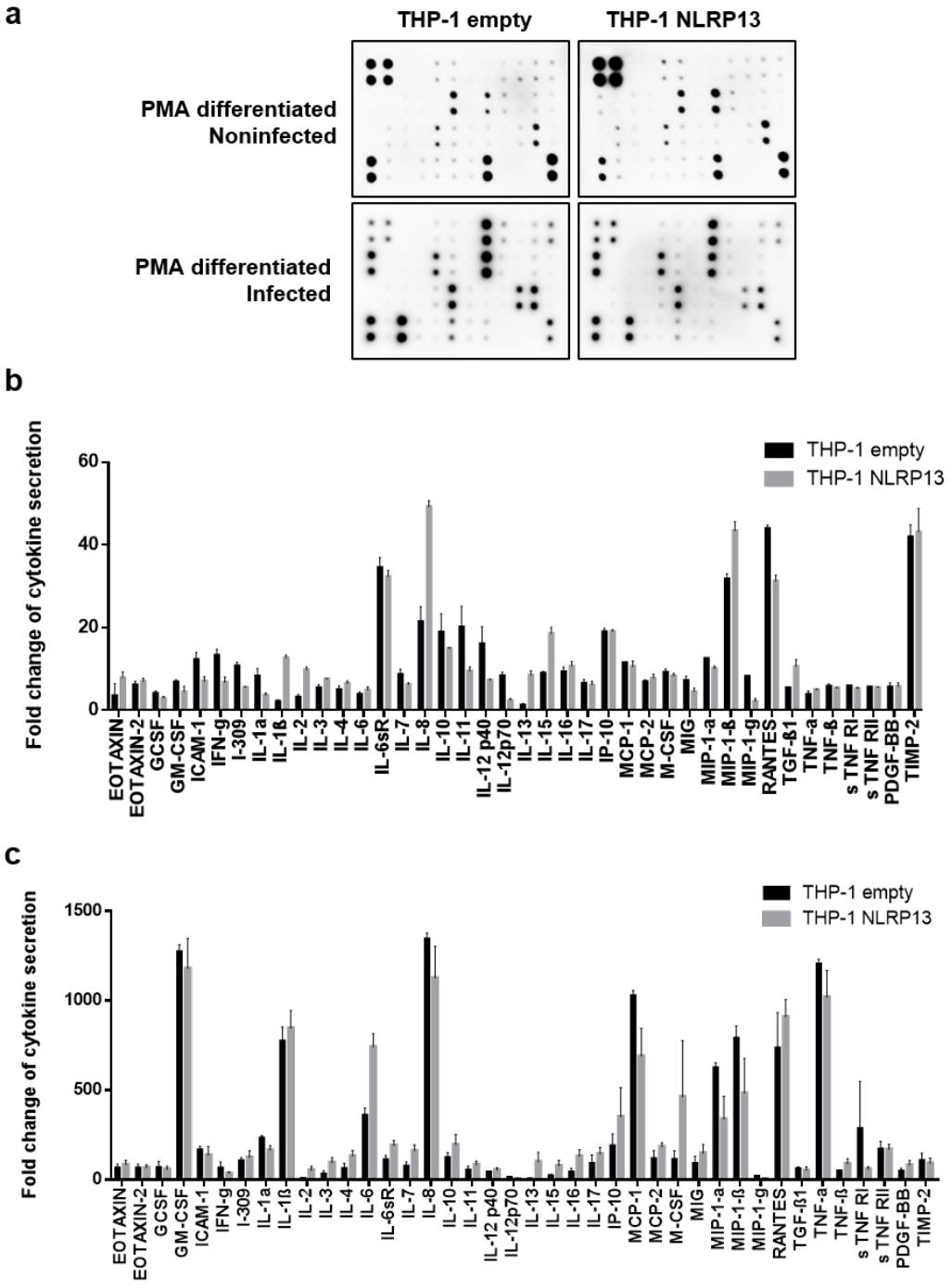

Figure 5.6. Cytokine secretion profile upon live infection with *P.aeruginosa* (MOI:10). (a) Human cytokine membrane array was used to detect cytokine profiling. (b,c) Intensity of cytokine dot blot array for noninfected (b) and infected (c) cells was calculated with Image-J. Mean ± SD

In order to examine the effects of infection eliminating PMA-derived consequences, stably-NLRP13 expressing THP-1 monocytes and control cells were infected with *P.aeruginosa* (MOI:10) without pre-PMA-differentiation and downstream cytokines of NLRP13 were studied. After 2 h infection, almost all of the monocytes became adherent. The supernatants were collected after 16 h infection. Secretion levels of IL-1β, TNF-α, and IL-6 were measured with ELISA. As seen in Figure 5.7, NLRP13 stable expression increases secretion levels of IL-1β, TNF-α, and IL-6 from 150, 1000, and 38 to 650, 2250, and 50 pg/ml, respectively. We might conclude that high levels of NLRP13 engender to statistically significant increase in secretion of these pro-inflammatory cytokines upon live infection with *P.aeruginosa*.

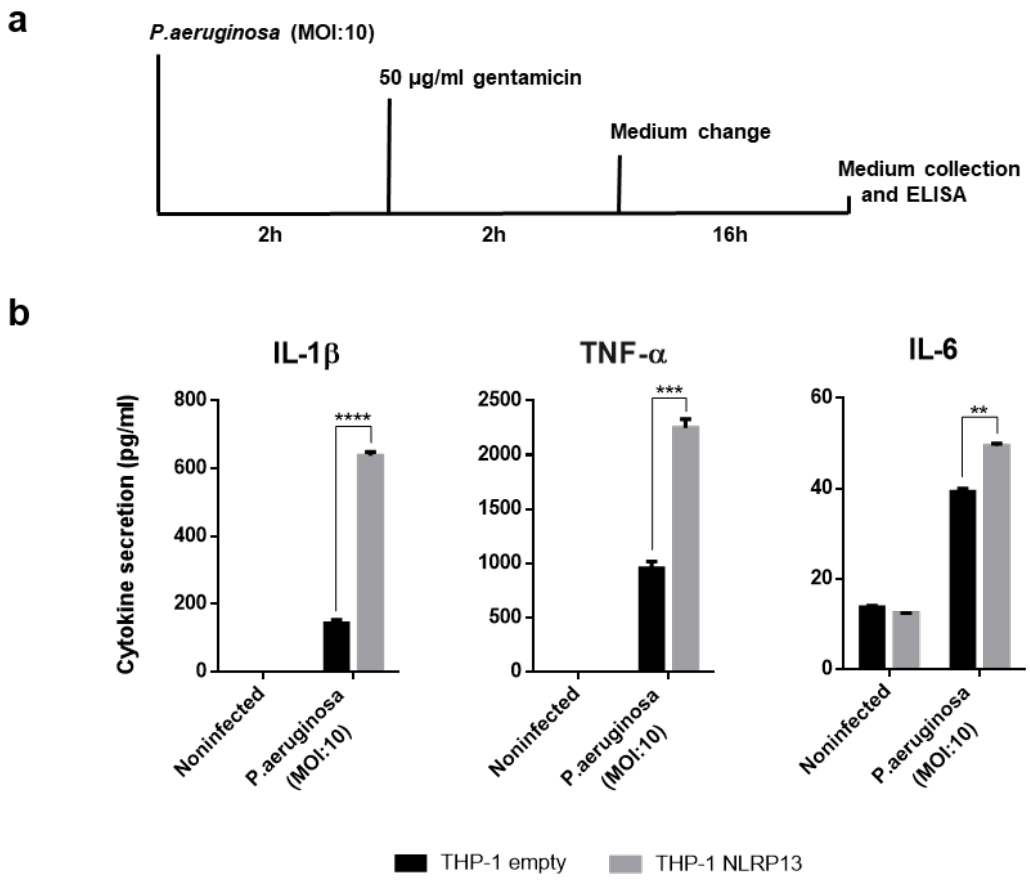

Figure 5.7. Increasing levels of NLRP13 positively affect secretion of pro-inflammatory cytokines upon live infection with *P.aeruginosa*.(a) Experimental procedure. (b) Levels of pro-inflammatory cytokine secretion were measured via ELISA. N=6; Multiple t-Test; **p<0.01; ***p<0.001; ****p<0.0001; mean ± SD

5.4.2. The Effects of NLRP13 on Inflammasome Activation

5.4.2.1. NLRP13 Changes Protein Levels of Inflammasome Components. We showed that increase in NLRP13 correlates with higher secretion of pro-inflammatory cytokines upon live infection with *P.aeruginosa*. We wondered how NLRP13 may affect protein levels of inflammasome components and activation of inflammatory caspases. In order to investigate this, stably-NLRP13 expressing THP-1 monocytes and control cells were infected with *P.aeruginosa*. Protein lysates and supernatants were collected at different time points and analyzed with WB and ELISA (Figure 5.8). We observed that *P.aeruginosa* infection caused statictically highly significant increase of pro-IL-1β level in stably-NLRP13 expressing THP-1 cells compared to control cells.

Consistent with increased pro-IL-1β level, secretion of IL-1β was enhanced by NLRP13 overexpression in a time-dependent manner. Elevated secretion of IL-1β indicates positive regulation of inflammasome activity by NLRP13. As expected, maturation of pro-Casp-1 was increased with high levels of NLRP13; enzymatically active p10 and p20 subunits of Casp-1 were detected much more in stably-NLRP13 expressing THP-1 cells than control cells. Furthermore, NLRP3 level increased upon infection in a time-dependent manner as known from literature. Interestingly, high levels of NLRP13 enhanced the increase in protein level of NLRP3 upon infection. In addition, stably-NLRP13 expressing THP-1 monocytes express higher level of ASC than control cells in the non-infected state.

We did not performed any viability or cell death assay; however, under microscope we observed infected cells underwent cell death over time. That is why samples for infected cells have lower total β-actin levels than samples for non-infected ones. Nevertheless, the protein levels of each samples were normalized to their corresponding β-actin levels.

Apart from Casp-1, the effects of NLRP13 on activation of Casp-8 upon *P.aeruginosa* infection were investigated (Figure 5.9a). Similar with ASC, higher level of p30

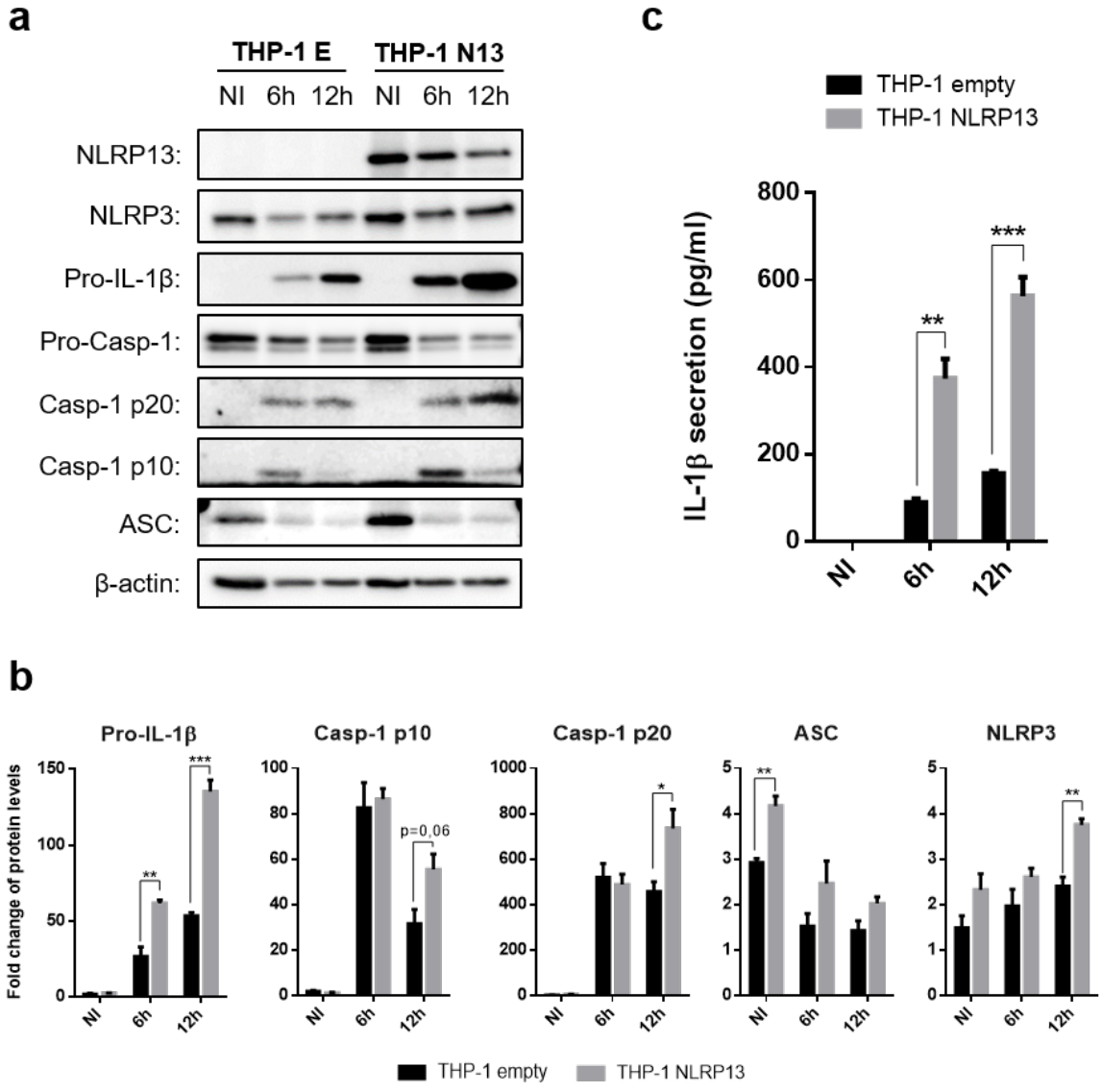

Figure 5.8. The effects of NLRP13 on protein levels of inflammasome components upon *P.aeruginosa* infection (MOI:10). (a) Protein levels of inflammasome components were analyzed with WB. (b) Quantification of WB. (c) IL-1β secretion. NI:Noninfected. N=3; Multiple t-Test; *p<0.05; **p<0.01; ***p<0.001; mean ± SD

subunit of Casp-8 was detected in stably-NLRP13 expressing THP-1 monocytes than control cells in the non-infected state. We could not detect p18 subunit of Casp-8; however, p10 subunit of Casp-8 was observed as increased with NLRP13 upon infection. Besides, increasing protein level of MALT1 upon infection was positively affected by NLRP13. Interestingly, NLRP13 protein level seems to decrease upon infection in a

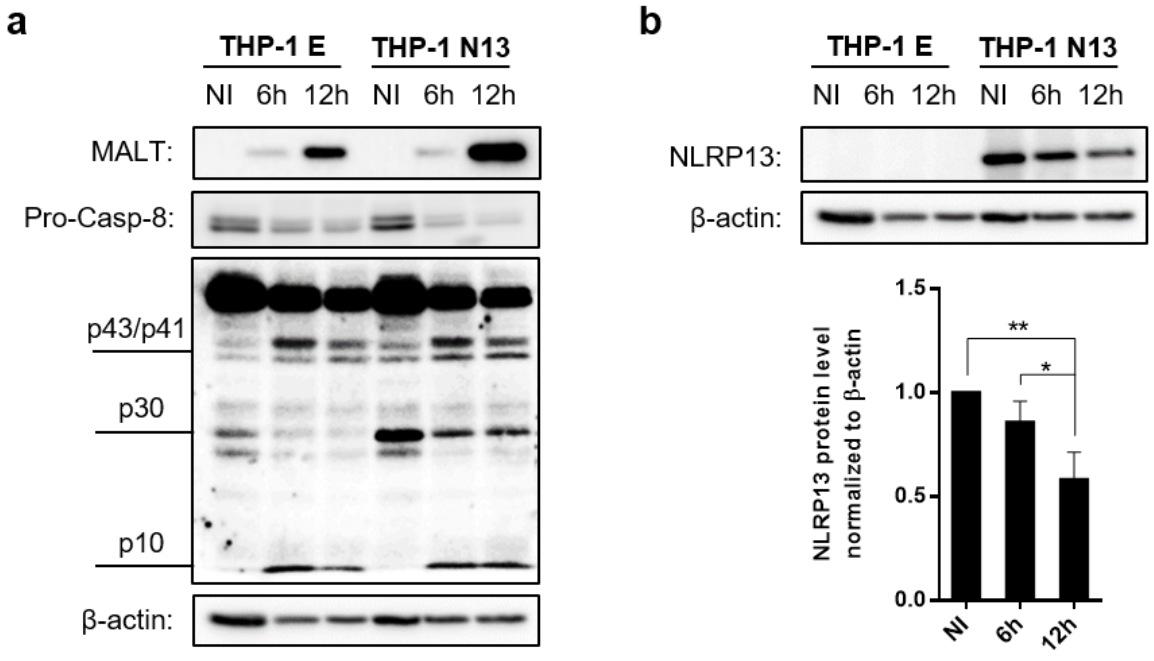

Figure 5.9. The effects of NLRP13 on of inflammasome components upon *P.aeruginosa* infection.(a,b) Protein levels of non-canonical inflammasome components (a) and NLRP13 (b) were analyzed with WB. NI:Noninfected. N=3; One-way ANOVA; *p<0.05; **p<0.01; mean ± SD

time-dependent manner (Figure 5.9b).

5.4.2.2. NLRP13 changes mRNA levels of inflammasome components. NLRP13 seems to increase protein levels of inflammasome components upon infection with *P.aeruginosa*. In order to inspect the effects of NLRP13 on mRNA levels of these molecules, THP-1 monocytes which stably expresses NLRP13 and empty vector were infected with *P.aeruginosa*. At 6th hour after infection, total RNA of the cells was isolated and converted into cDNA. Gene expression of inflammatory molecules was analyzed by q-RT-PCR and fold changes were measured as normalizing each gene expression to GAPDH expression. As seen in Figure 5.10, *P.aeruginosa* led to statistically significant increase in mRNA level of endogenous NLRP13. Increasing NLRP13 levels resulted in increased expression of IL-1β and IL-6 and decreased expression of pro-Caspase-1 and ASC.

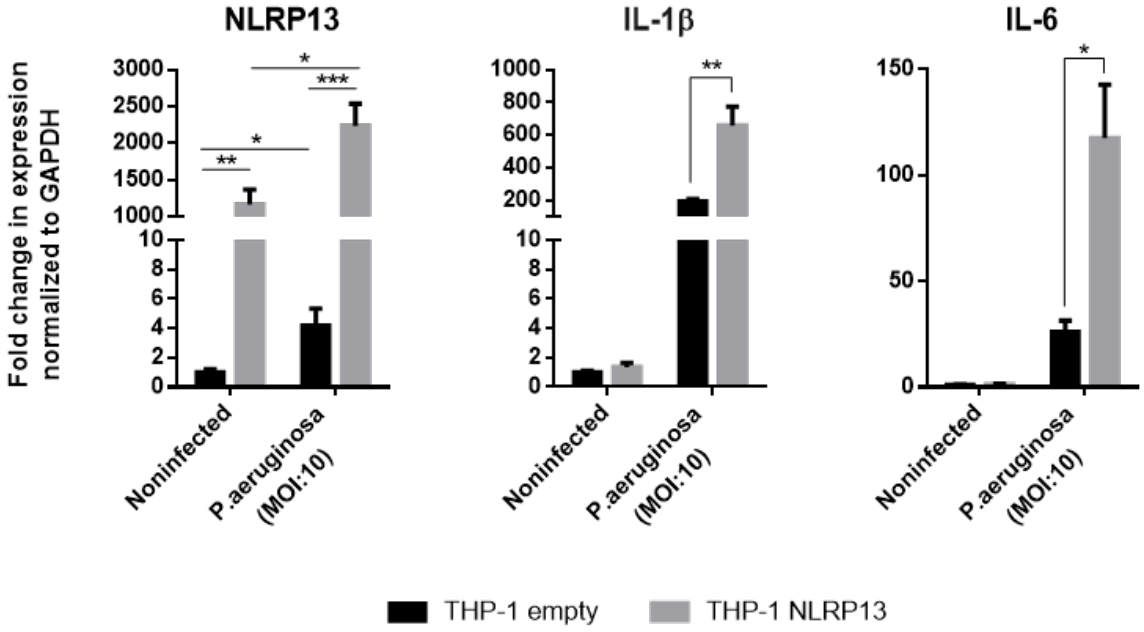

Figure 5.10. The influence of NLRP13 on expression of inflammasome components upon *P.aeruginosa* infection. Gene expressions was analyzed via q-RT-PCR and normalized to GAPDH. N=3; Multiple t-Test; *p<0.05; **p<0.01; ***p<0.001; ****p<0.0001; mean ± SD

5.4.2.3. Knock-down of NLRP13 Decreases Expression of IL-1β. For further examination of the roles of NLRP13 in inflammasome activation, we decided to generate NLRP13 knock-out THP-1 cells via CRISPR-Cas9 system. To do that, guide RNAs against NLRP13 were designed and cloned in pLKO-5-sgRNA-EFS-GFP plasmid. The success of cloning was verified via Sanger Sequencing. Since transduction efficiency is low in THP-1 monocytes, NLRP13-knock out Hec1A cells were concurrently generated to see which guideRNA works. Hec1A was chosen for this purpose because endogenous expression of NLRP13 is high in this cell line. Before transduction with sgRNA containing lentiviruses, cell lines were generated by lentiviral transduction for stable expression of dox-inducible Cas9 (DIC9) (Figure 5.11a and 5.12a). Then, the stably-DIC9 expressing cells were transduced with guide RNA-containing viruses. The cells which were positive for guide RNA were sorted by GFP construct on the plasmid (Fig-

ure 5.11b and 5.12b,c). Successful generation of NLRP13-knock out Hec1A cell line with guide RNA 6 was observed with WB (Figure 5.11c). However, this guide RNA did not work on THP-1 cell alone. Thus, ThP-1 DIC9 cells were transduced with pool of guide RNA 1, 3, and 6 against NLRP13. In this case, knock-down of NLRP13 in THP-1 cells were detected via q-RT-PCR (Figure 5.12d). Additionally, it was observed that NLRP13-knock down in THP-1 cells results in diminished expression of IL-1β upon *P.aeruginosa* infection.

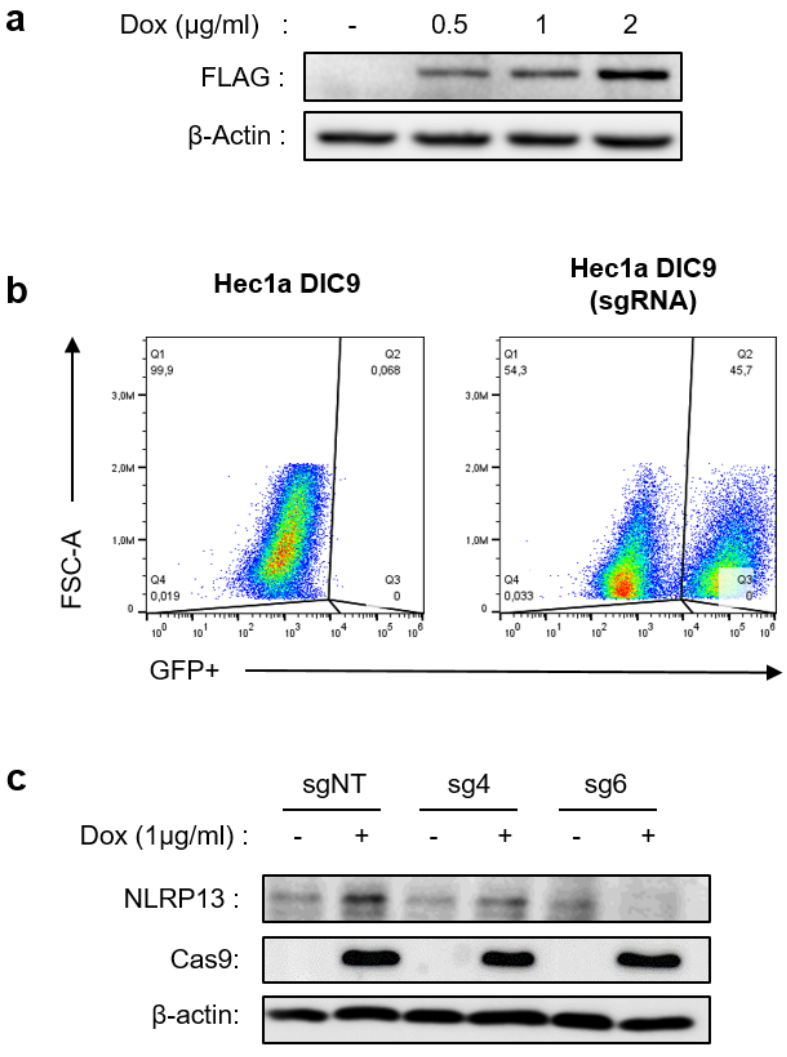

Figure 5.11. Generation of NLRP13-knock out Hec1A Cell Line. (a) Expression of DIC9 was detected with anti-FLAG ab. (b) Sorting of Hec1A DIC9 cells transduced with sgRNA. (c) NLRP13 levels were detected via WB.

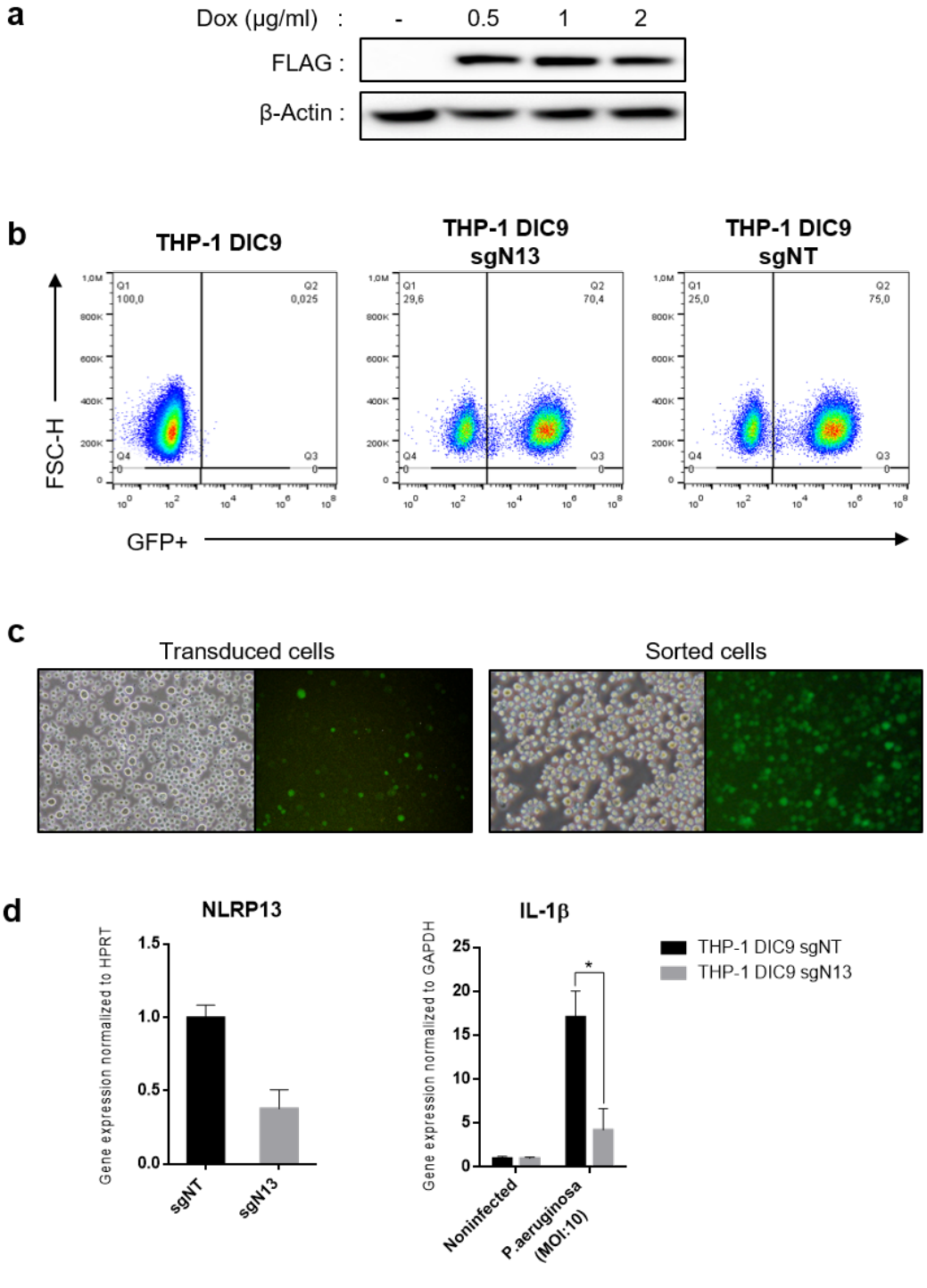

Figure 5.12. NLRP13-knock down negatively affects IL-1β expression upon *P.aeruginosa* infection (a) Generation of THP-1 DIC9 was verified with anti-FLAG ab. (b,c) Sorting of THP-1 DIC9 cells transduced with sgRNA. (d) NLRP13 and IL-1β levels were detected via q-RT-PCR. N=3; Multiple t-Test; *p<0.05; mean ± SD

5.4.3. The Effects of NLRP13 on AKT, ERK, and NF-κB pathways

The effects of NLRP13 on AKT, ERK, and NF-κB pathways upon *P.aeruginosa* infection were studied, since these pathways are critical for cell survival/death, macrophage differentiation, and inflammatory response. THP-1 monocytes were infected with *P.aeruginosa* (MOI:10). Protein lysates were collected at 6th and 12th hour of infection and analyzed with WB (Figure 5.13). We observed that NLRP13 overexpression contributes to statistically significant increase in phosphorylation of IκB-α upon infection. Interestingly, phosphorylation of AKT was diminished with NLRP13, while phophorylation of ERK was not affected.

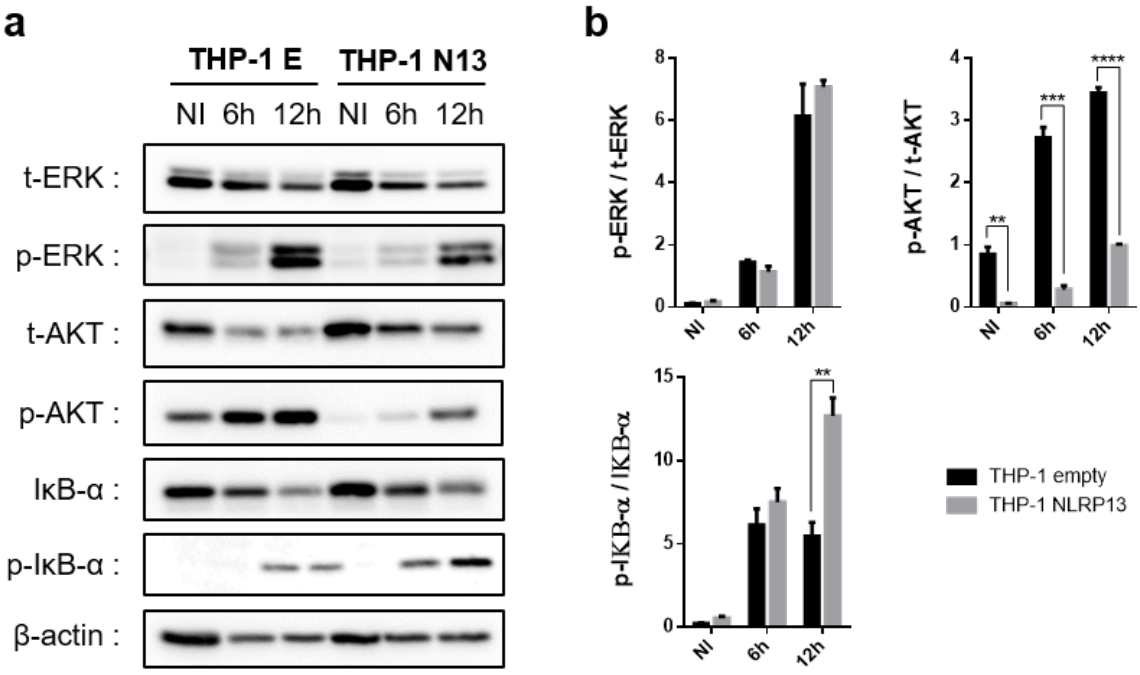

Figure 5.13. NLRP13 enhances IκB-α phosphorylation while diminishes AKT phosphorylation upon *P.aeruginosa* infection. (a) Protein levels were analyzed with WB. (b) Quantification of WB results. NI:Noninfected, E:empty, N13:NLRP13. N=3; Multiple t-Test; **p<0.01; ***p<0.001; ****p<0.0001; mean ± SD

5.5. The Role of NLRP13 in Macrophage Differentiation

5.5.1. The Effects of NLRP13 on Macrophage Surface Markers

We observed NLRP13 increases M-CSF secretion upon *P.aeruginosa* infection, when profiling cytokine secretions via human cytokine membrane array (Figure 5.6). In line with the thesis of Yalçınkaya, in which NLRP13 was suggested to be cleaved by Casp-8 and Casp-9 and knowledge from literature about the role of Casp-8 in macrophage differentiation [31], we addressed the question whether NLRP13 may have a role in macrophage differentiation.

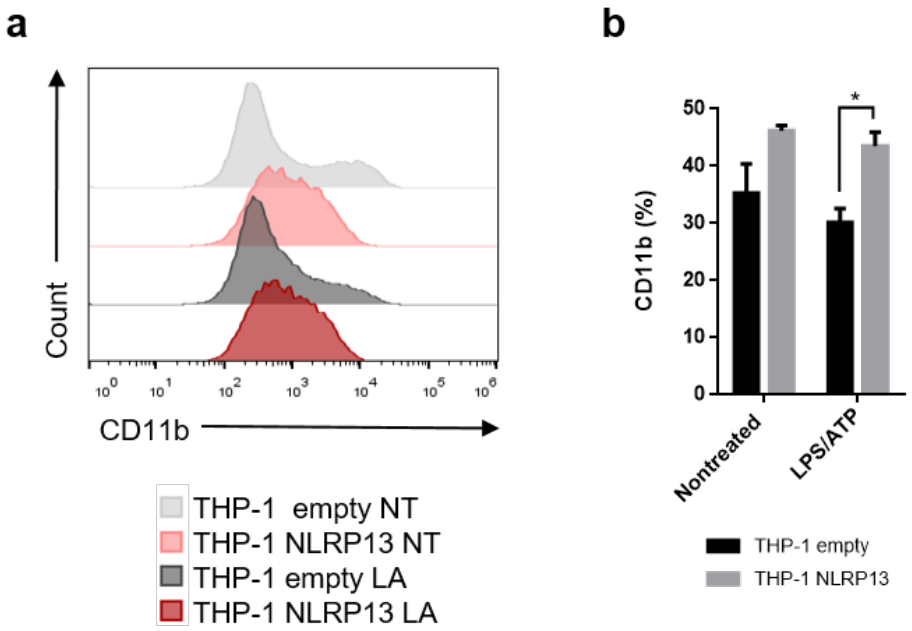

Figure 5.14. NLRP13 enhances the expression of CD11b. (a) The expression of CD11b in PMA-differentiated and LPS/ATP-treated cells was detected with flow cytometry after surface staining. (b) Percentage of CD11b positive cells. NT:Nontreated; LA:LPS/ATP. N=3; Multiple t-Test; *p<0.05; mean ± SD

In order to investigate this, stably-NLRP13 expressing THP-1 cells and control cells were differentiated with 100 ng/ml PMA for 9h and the media of cells were changed. The cells were allowed to differentiate for three days. Then, the cells were

treated with LPS/ATP and the surface staining against CD11b, a macrophage marker, was performed. Flow cytometric analyses showed that NLRP13 overexpression correlates with increasing population of $CD11b^+$ cells with LPS/ATP treatment (Figure 5.14).

Apart from CD11b, expressions of CD80 (M1 marker) and CD163 (M2 marker) expression were analyzed via FC (Figure 5.15). Like CD11b, the ratio of $CD80^+$ cells was increased by NLRP13 upon LPS/ATP treatment. Interestingly, CD163 expression was significantly increased in stably-NLRP13 expressing THP-1 cells with only extended PMA-differentiation. After LPS/ATP treatment, CD163 expression slightly decreased.

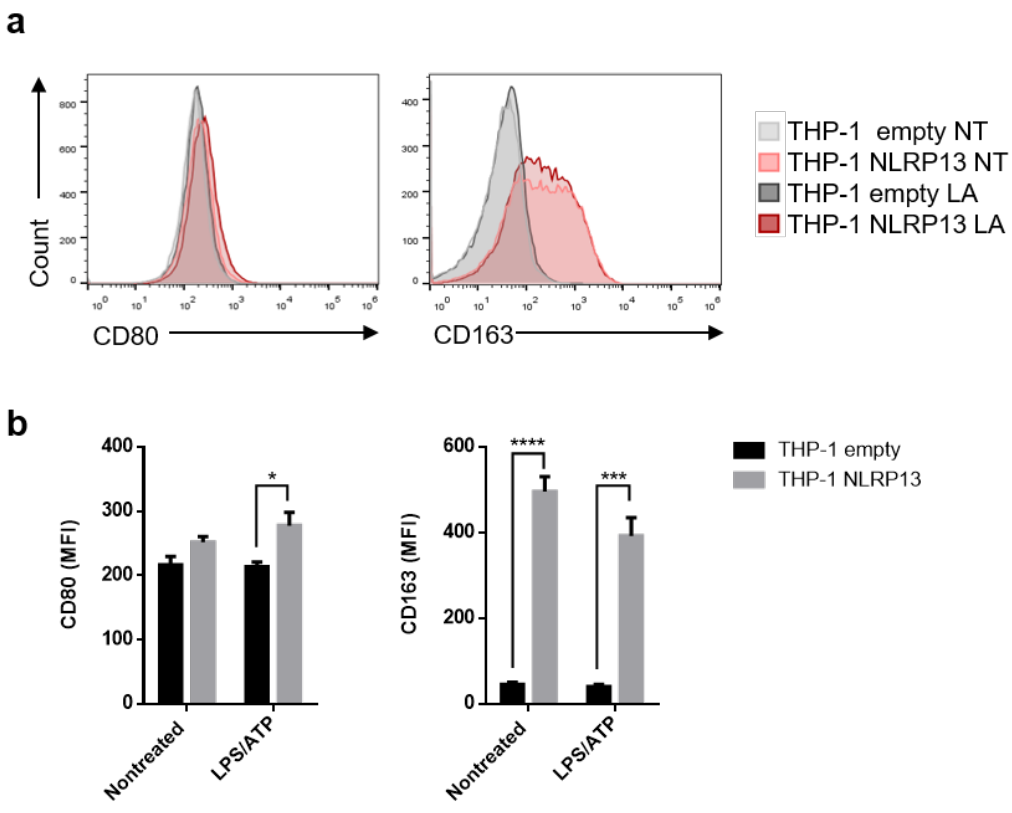

Figure 5.15. The effects of NLRP13 on macrophage polarization.(a) The expression of CD80 and CD163 in PMA-differentiated and LPS/ATP-treated cells was detected with flow cytometry. (b) MFI of CD80 and CD163. NT:Nontreated; LA:LPS/ATP. N=3; Multiple t-Test; *$p<0.05$;***$p<0.001$; ****$p<0.0001$; mean ± SD

5.5.2. The Effects of NLRP13 on AKT and ERK phosphorylation

Since AKT and ERK pathways are essential for macrophage differentiation, we investigated the effects of NLRP13 on AKT and ERK phosphorylation in PMA- differentiated THP-1 cells. 9h PMA-differentiation protocol was performed. Two days after differentiation, stably-NLRP13 expressing macrophages and control cells were primed with LPS for 3h and treated with ATP for 30 min. The results of WB showed that NLRP13 overexpression increases phosphorylation of AKT and ERK during PMA-differentiation (Figure 5.16). Only LPS treatment did not change the effect of NLRP13 on phosphorylation of these proteins; whereas ATP treatment along with LPS dramatically decreased the levels of p-ERK and p-AKT, as seen in last two lanes. Despite of the negative impact of ATP on activation of ERK and AKT, the levels of p-ERK and p-AKT were higher in stably-NLRP13 expressing THP-1 macrophages compared to control cells.

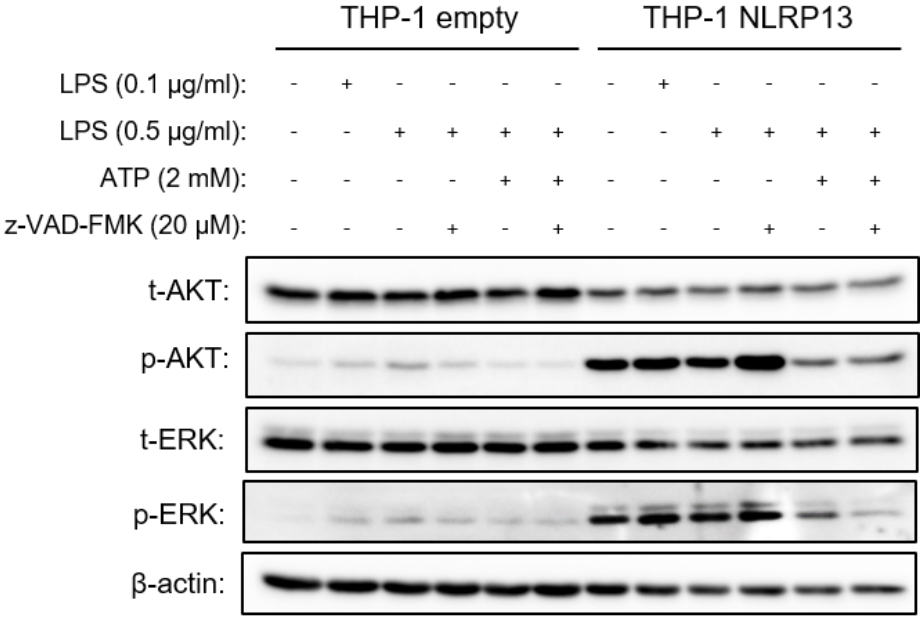

Figure 5.16. Extended PMA differentiation increases phosphorylation of AKT and ERK in stably-NLRP13 expressing cells. The cells were differentiated with 100 ng/ml PMA for 9h, two days later, treatments were performed. Protein levels of t-ERK, p-ERK, t-AKT, p-AKT, and β-actin were detected with WB.

5.5.3. The Effects of Extended PMA-differentiation on NLRP13-drived Secretion of IL-1β

We observed that PMA-differentiation raises CD163 expression of stably-NLRP13 expressing THP-1 cells. Previous infection data showed that 3h PMA differentiation before infection diminishes the positive effect of NLRP13 on secretion of pro-inflammatory cytokines compared to infection of monocytes, although high levels of NLRP13 still contributes to statistically significant increase of secretion levels. In order to examine whether these consequences are related with PMA-differentiation, IL-1β secretion of 9h PMA-differentiated macrophages and non-differentiated monocytes was compared after *P.aeruginosa* infection (Figure 5.17). Extended PMA-differentiation dramatically reduced the positive effect of NLRP13 on IL-1β secretion against *P.aeruginosa*. As previously shown, stably-NLRP13 expressing THP-1 cells which were infected without PMA-differentiation secretes significantly higher levels of IL-β than control cells, whereas there was not any significant difference between these two cell lines in the case of extended PMA-differentiation followed by infection.

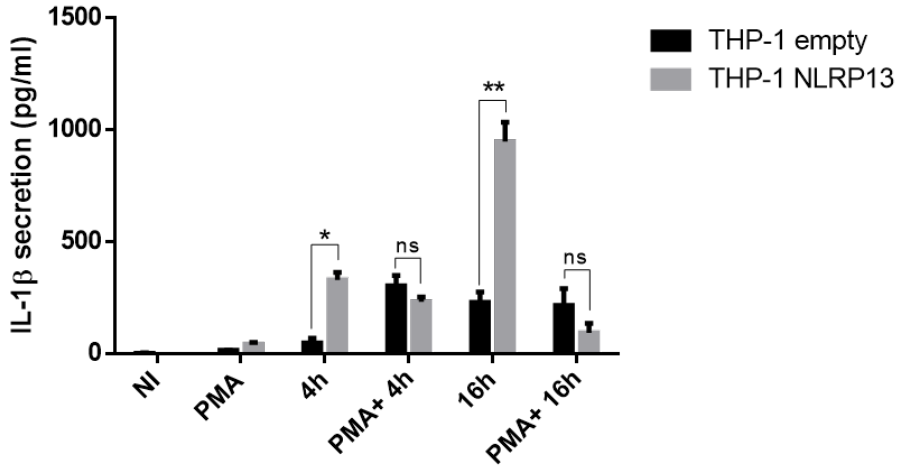

Figure 5.17. Extended PMA-differentiation cancels the positive effect of NLRP13 on IL-1β secretion upon *P.aeruginosa* infection. Secretion of IL-1β was measured via ELISA. NI:noninfected. N=3; Multiple t-Test; ns:not significant; *p<0.05;**p<0.01; mean $\pm$ SD

5.5.4. The Effects of NLRP13 on Expression of M1, M2, and DC Markers

The difference of consequences of NLRP13 overexpression between undifferentiated and differentiated cell lines during infection brings the questions whether high levels of NLRP13 cause THP-1 monocytes to differentiate into dendritic cells in *P.aeruginosa* infection. To answer this question, THP-1 monocytes were infected and expression of DC markers were analyzed with q-RT-PCR (Figure 5.18). Contrary to what was thought, high levels of NLRP13 did not affect the expression of CD1c, conventional DC marker. Indeed, NLRP13 engendered decrease in expression of BCDA2, plasmacytoid DC marker, upon infection. Additionally, the expression of CCR7 and CD206, which are M1 and M2 marker respectively, were not altered by NLRP13 level.

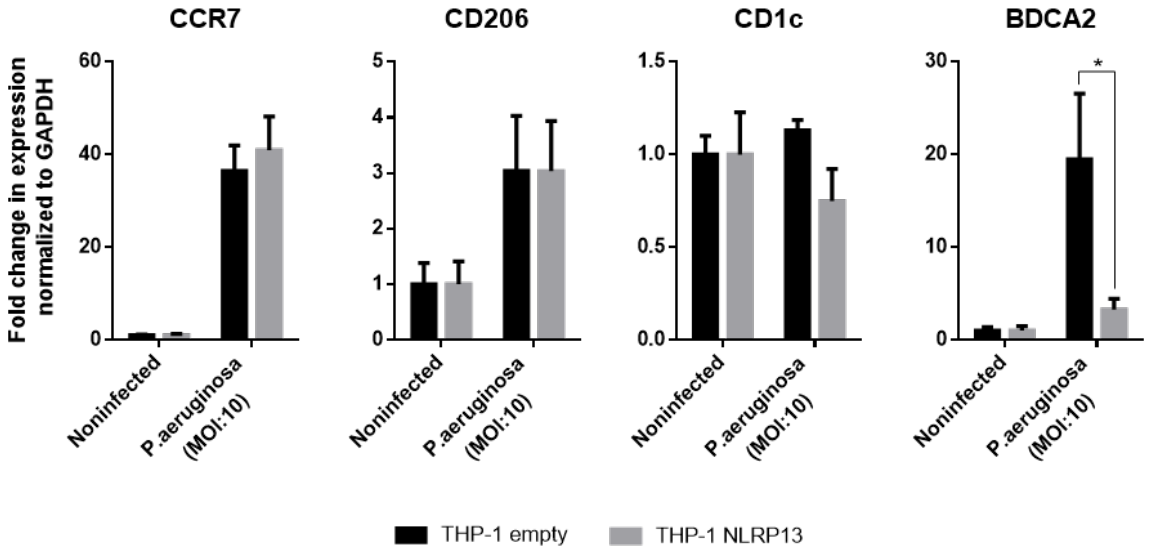

Figure 5.18. The influence of NLRP13 on expression of M1, M2, and DC markers upon *P.aeruginosa* infection. THP-1 monocytes were infected with *P.aeruginosa* and gene expression of CCR7, CD206, CD1c, and BDCA2 was analyzed via q-RT-PCR. N=3; Multiple t-Test; *p<0.05; mean ± SD

5.6. Post-translational cleavage of NLRP13 by Caspase-8

5.6.1. LPS-treatment Leads to Cleavage of NLRP13 in THP-1 cells.

Through the experiments, where the role of NLRP13 in inflammasome activity after LPS and ATP treatments was examined, a cleaved band around 70 kDa was observed using the monoclonal anti-NLRP13 ab (Figure 5.19). This band was detected with homemade monoclonal anti-NLRP13 antibody (2c11) in the PMA-differentiated stably-NLRP13 expressing THP-1 cells which were treated with LPS/ATP. Interestingly, the cleavage of NLRP13 was inhibited by pan-caspase inhibitor z-VAD-FMK. As can be seen from lanes 7 and 8, no cleaved products can be observed upon caspase inhibition.

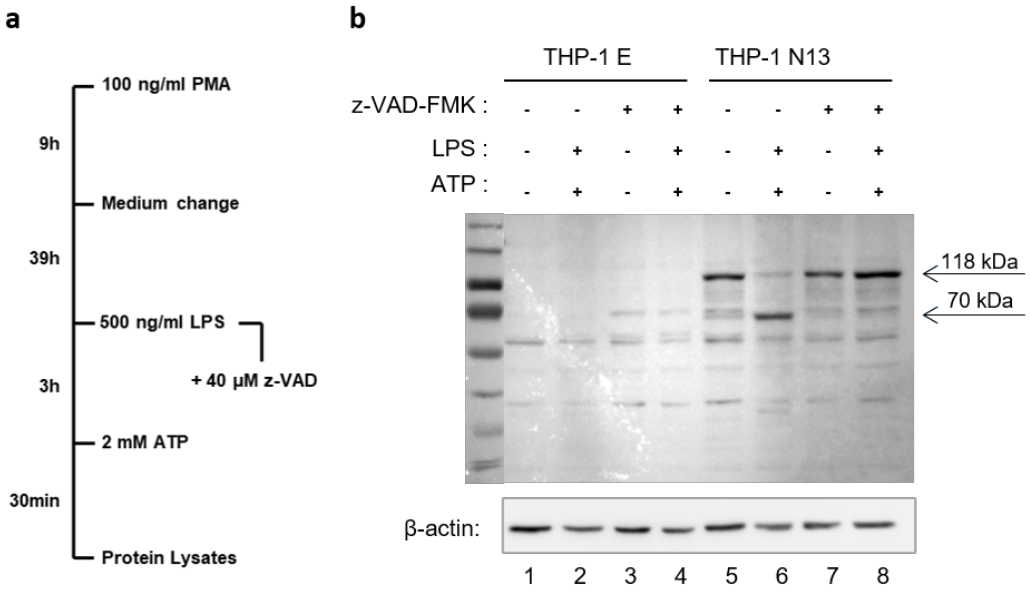

Figure 5.19. LPS treatment results in post-translational cleavage of NLRP13. (a) Experimental procedure. (b) NLRP13 protein level was detected with 2c11 ab. β-actin was used as loading control. E:empty; N13:NLRP13

According to thesis of Yalçınkaya, NLRP13 is processed by Casp-8 and Casp-9. When it was co-transfected with these caspases into HEK293-FT cells, around 40

kDa clevage product was observed in WB. Moreover, when NLRP13 was transfected with enzymatically inactive mutants of Casp-8 and Casp-9, the cleavage product was not detected. Considering possible roles for Casp-8 in inflammasome signaling and macrophage differentiation, we decided to further investigate the cleavage of NLRP13 by Casp-8. Firstly, we showed NLRP13 interacts with Casp8 with co-IP (Figure 5.20). NLRP13 was co-transfected with either pcDNA3, HA-Casp-8, or mutant HA-Casp-8 in HEK293-FT cells. Then, Casp-8 was pulled down by anti-HA ab. When checking the interaction between Casp8 and NLRP13 via WB, NLRP13 protein level were observed to decrease with HA-Casp-8 in whole cell lysates (Lane 5) and NLRP13 was not pulled down with HA-Casp8 (Lane 2). However, if enzymatically mutant version of HA-Casp-8 was used, NLRP13 was successfully pulled down with Casp-8 (Lane 3). Therefore, it could be concluded that NLRP13 interacts with Casp-8. To figure out cleavage process of NLRP13, we decided to perform *in vitro* cleavage assay. Therefore, purification of NLRP13 was required.

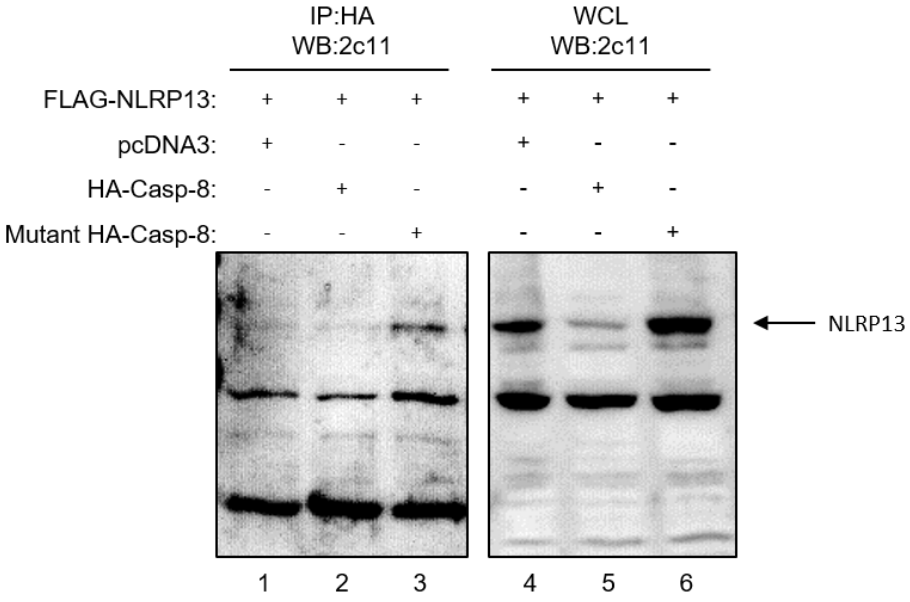

Figure 5.20. NLRP13 interacts with Casp-8. NLRP13 was co-transfected with either pcDNA3, HA-Casp-8, or mutant HA-Casp-8 in HEK293-FT cells. Casp-8 was immunoprecipitated and NLRP13 was detected via WB.IP: Immunoprecipitation; WCL: Whole cell lysates.

5.6.2. Production and Purification of NLRP13 for Further Assays

In order to purify NLRP13, we firstly planned to produce NLRP13 by IPTG-induction in PET-30a expression system and purify it using His-Trap Protein Purification Columns. NLRP13 was successfully produced in Rosetta-pLysS *E.coli* strain by 8h IPTG-induction at 18°C, as seen in Figure 5.21a. After production of NLRP13, bacteria were sonicated and the obtained supernatant was loaded into His-Trap columns. However, the purification of NLRP13 was not successful and there was no detectable NLRP13 protein either in the elution or flow-through samples.

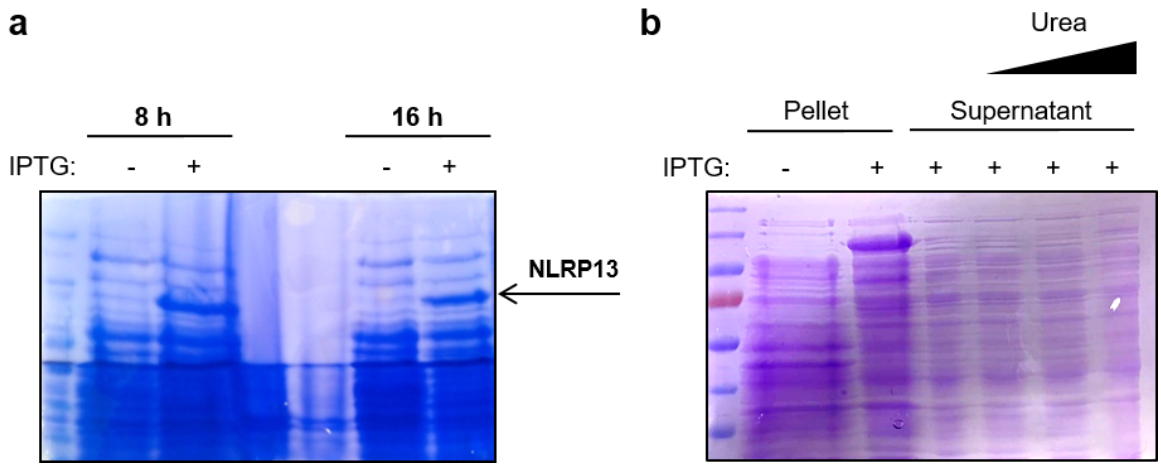

Figure 5.21. Production of NLRP13 by IPTG-induction. (a) NLRP13 production by IPTG-induction was verified with Coomassie Blue Staining. (b) After production, NLRP13 was observed to precipitate as inclusion bodies.

When the pellet and supernatant of sonicated bacteria were examined via Coomassie Blue staining, NLRP13 was observed in the pellet (Figure 5.21b) that indicates NLRP13 aggregates in the inclusion body. Then, different concentration of Urea up to 8 M was used to solubilize the inclusion body, without any progress. Apart from Urea, 0.75 M potassium chloride, 3.2 M EDTA, 4.8 M guanidinium chloride and different combinations of these chemicals were used to solubilize the inclusion body; however, they were not sufficient to rescue NLRP13 from the pellet. Thus, we decided to purify NLRP13 from polyacrylamide gel according the protocol optimized by Yalçınkaya.

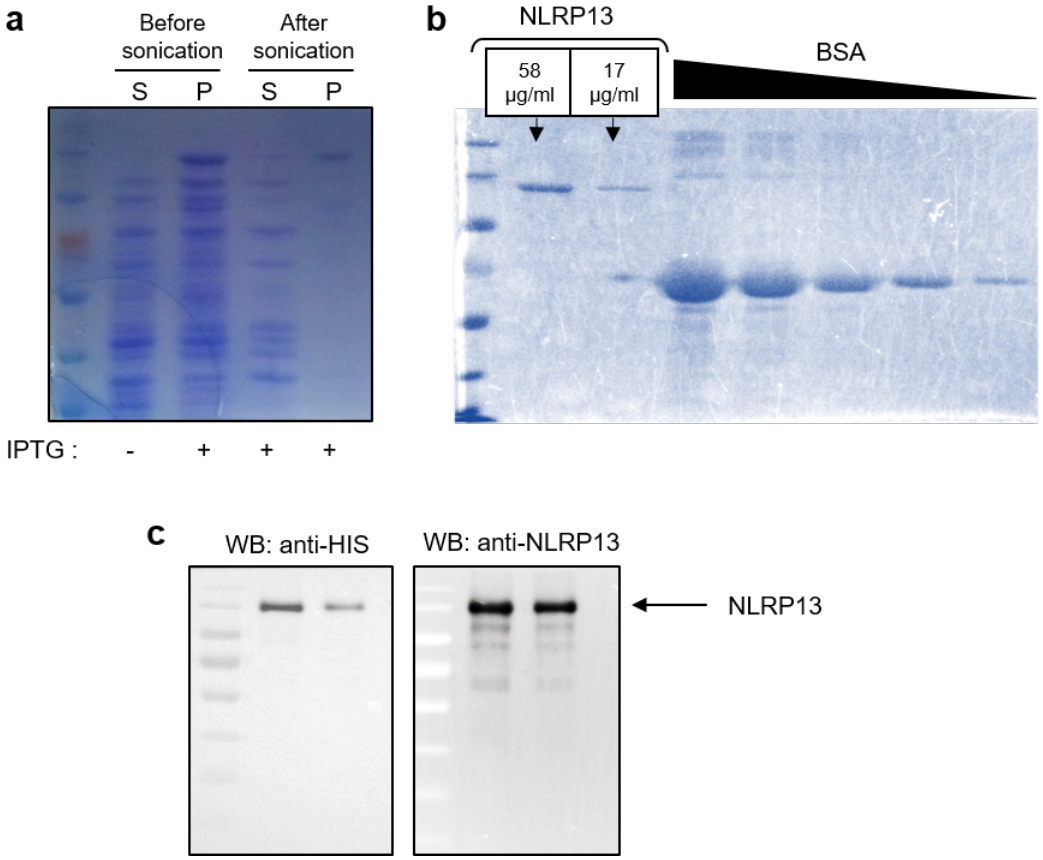

Figure 5.22. Purification of NLRP13 from polyacrylamide gel. (a) Triton-X100 precipitation of NLRP13 in pellet was observed by Coomassie Blue staining. (b) Amount of NLRP13 purified from gel slices was calculated by comparing BSA standards. (c) Purified NLRP13 was validated via WB. S:Supernatant; P:Pellet

In this protocol, NLRP13 was precipitated into the pellet instead of recovery from pellet using Triton X-100 which provides elimination of soluble proteins from pellet (Figure 5.22a). Then, the samples were run on SDS-PAGE and NLRP13 was purified by cutting corresponding part of gel. In order to check the success of purification and calculate the amount of protein, purified NLRP13 together with BSA standards was run and stained with Coomasie Blue (Figure 5.22b). The concentrations of first and second samples were calculated as 58 and 17 μg/ml using Image-J. The purified samples were analyzed with WB for validation of whether the purified protein was actually NLRP13. Successfully purified NLRP13 was detected with anti-NLRP13 and

anti-HIS antibodies (Figure 5.22c).

5.6.3. *In vitro* Cleavage Assay of NLRP13 with Recombinant Human Casp-8

Purified NLRP13 was cleaved by recombinant human caspase-8. Samples of the cleavage reaction were analyzed via WB. As shown in Figure 5.23, casp-8 resulted in a cleaved band about 40 kDa which was not detected in negative controls. This cleavage product was detected with both anti-HIS and anti-NLRP13 antibody (Lanes 2, 4, 6, and 8). Since anti-NLRP13 is a polyclonal antibody, other cleaved bands around 70 and 55 kDa were detected only with this antibody (Lanes 6 and 8).

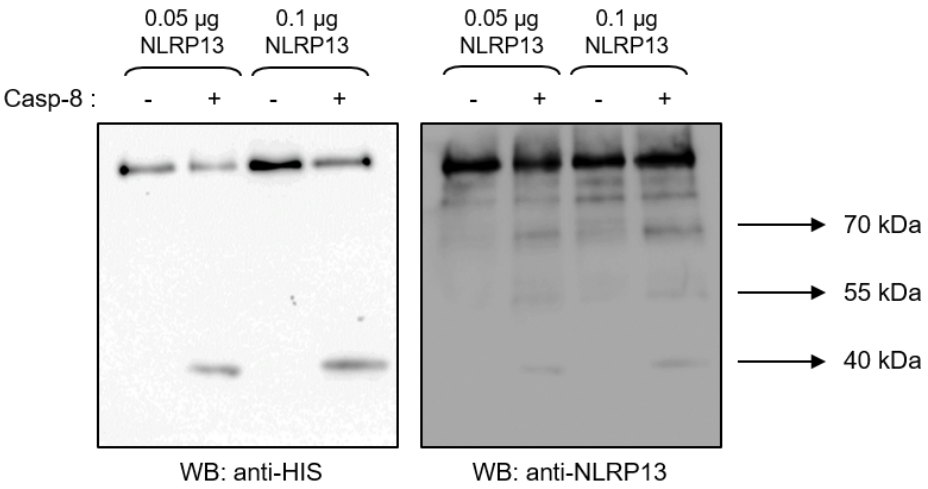

Figure 5.23. *In vitro* cleavage assay of NLRP13 with recombinant human Caspase-8. 0.05 and 0.1 μg of purified NLRP13 were cleaved with 1U recombinant human Caspase-8. Cleaved forms of NLRP13 was detected via WB.

6. DISCUSSION

NLRP13 is a primate specific member of the NLR family containing PYRIN domain. In the literature, NLRP13 was mentioned only in two papers. In one of them, the expression of NLRP13 in THP-1 macrophages was observed to be upregulated by *Toxoplasma gondii* infection [26]. The other suggested that U87 glioblastoma cells, which are resistant to doxorubicin in an *in vitro* tumor microfluidic ecology, has a missense mutation in the NLRP13 gene [27]. These findings were not sufficient to understand the function of NLRP13 in inflammasome activity. Fortunately, the pioneering theses of Yetiş Gültekin [**?**] and Mustafa Yalçınkaya [**?**] have enriched our knowledge about NLRP13 significantly. From Gültekin Y., we know that NLRP13 is mainly localized in the cytoplasm and partially in mitochondria (%35). Gültekin Y. showed that NLRP13 weakly interacts with Caspase-1 and ACS via co-immunoprecipitation experiments. He also observed that NLRP13 forms inflammasome-like structures with ASC and Caspase-1 under overexpression conditions, but NLRP13 has no dose dependent effect on the numbers of ASC speck formation. Then, Yalçınkaya M. showed that the protein level of NLRP13 is upregulated with LPS/ATP treatment in THP-1 macrophages and NLRP13 was recruited to ASC specks as response to treatment with LPS/ATP. Yalçınkaya M. also observed that NLRP13 protein levels are reduced when it is co-transfected with Casp-8 and Casp-9 in HEK293FT cells.

In line with these findings and general knowledge about the NLR family from literature, we aimed to investigate NLRP13-driven innate immune response. Firstly, we examined the NLRP13 dependent cytokines upon 3h PMA differentiation followed by LPS/ATP treatment. We observed that NLRP13 overexpression lead to increase in the protein level of pro-IL-1β. In addition, stable expression of NLRP13 positively regulates secretion of pro-inflammatory cytokines IL-1β and TNF-α, while negatively regulates secretion of anti-inflammatory IL-10 upon LPS/ATP treatment (Figure 5.2 and 5.3). These data suggest that NLRP13 acts as pro-inflammatory cytoplasmic sensor in response to LPS and ATP stimulation. Interestingly, with the experiment of

extended PMA-differentation followed by LPS and ATP treatment, only LPS treatment was inspected to change the secretion levels of cytokines as higher as LPS/ATP treatment in stably-NLRP13 expressing cells. It could be suggested that NLRP13 inflammasome may be activated in response to only LPS.

The pro-inflammatory effect of NLRP13 after LPS and ATP stimulation was augmented with extended PMA-differentiation. This could be reasoned by cumulative activity of PMA and NLRP13 on the activation of the ERK pathway, since we observed that NLRP13 overexpression increased phosphorylation of ERK through macrophage differentiation and LPS/ATP treatment. Besides, we know that PMA is a strong activator of the Ras-ERK pathway from the literature. PMA is a membrane-permeable ester which could directly bind Protein Kinase C and activate it mimicking its ligand. Activated Protein Kinase C pathway enhances the activation of MAPK-ERK [33] which is essential for macrophage survival.

Apart from LPS and ATP, we examined the pathogen-specific involvement of NLRP13 in innate immune response. LPS is the major component of the outer membrane of gram-negative bacteria. NLRP13 overexpression significantly increases secretion of pro-inflammatory cytokines. Accordingly, we considered that NLRP13 may have a role against gram-negative bacteria. 3h PMA-differentiated THP-1 macrophages were infected with *S.aureus* and *P.aeruginosa* which are gram-positive and gram-negative, respectively. Interestingly, NLRP13 overexpression increased the secretion of IL-1β upon *P.aeruginosa* infection, whereas it did not affect *S.aureus*-specific secretion of IL-1β. Consistent with the secretion of IL-1β in the results of bead array, protein levels of pro-IL-1β were significantly increased by stable expression of NLRP13 in THP-1 cells infected with *P.aeruginosa*, while there is no significant difference in *S.aureus*-infected cells. Thus, it is clear that NLRP13 gives rise to pathogen-specific activity against *P.aeruginosa*, but not *S.aureus*.

To study *P.aeruginosa*-specific activity of NLRP13 on the maturation IL-1β, we further examined the effects of NLRP13 on inflammasome activation and cytokine reg-

ulation upon *P.aeruginosa* infection. We firstly screened the downstream inflammatory cytokine profile using a membrane based human inflammatory cytokine array. We observed that high expression of NLRP13 increases secretion of IL-1β, IL-6, IP-10, and M-CSF. IP-10 is a pro-inflammatory cytokine like IL-1β and IL-6; M-CSF is the one of the key factors for macrophage differentiation. Although the secretion levels were considerably low for PMA-differentiated control cells, NLRP13 affected the secretion levels of certain cytokines like IL-1β, IL-8, and MIP-1-β. In order to determine the effects of infection eliminating PMA-derived consequences, THP-1 monocytes were directly infected with *P.aeruginosa*. Indeed, PMA differentiation is established in the literature as classical method for priming cells to receive detectable response in case of treatments with PAMPs. Nonetheless, it is not necessary in the infection case, since the cells were stimulated with intact bacteria as a collective treatment including many PAMPs. We observed that stably-NLRP13 expressing THP-1 monocytes secreted considerably higher levels of IL-1β, TNF-α, and IL-6 compared to control cells in response to *P.aeruginosa*. In agreement with these findings, NLRP13 seems to act a pro-inflammatory cytoplasmic sensor against *P.aeruginosa*.

For further confirmation of our infection study, the effects of NLRP13 levels on protein and mRNA levels of inflammasome components were analyzed. Consistent with increased secretion of IL-1β, protein levels of pro-IL-1β were significantly elevated by higher levels of NLRP13. Likewise, maturation of pro-Casp-1 was enhanced by NLRP13 overexpression, we could detect both p10 and p20 which are active protease subunits of Casp-1 (Figure 5.8). These data indicate that NLRP13 activates assembly of inflammasome complex which results in cleavage of pro-IL-1β leading to its secretion.

Apart from maturation of pro-Casp-1, we detected positive correlation between NLRP13 levels and Casp-8 activation. Particularly, higher levels of the intermediary C-terminal cleavage product of Casp-8, p30, was detected in stably-NLRP13 expressing THP-1 monocytes than control cells. p30 subunit of Casp-8 consists of two protease subunits p10 and p18. Since p30 can be quickly processed into p10 and p18 by active caspases and it can be found in caspase-8 activating complexes, it amplifies activation

of Casp-8 [34]. Therefore, it could be thought that NLRP13 provides higher tendency to the activation of pro-Casp-8. In this regard, we observed NLRP13 overexpression results in increase of cleaved subunits p43/p41, p30 and p10 of Casp-8 upon infection. p18 subunit was not detected; however, increase of p43/41 and p10 and decrease of p30 shows activation of pro-Casp-8. In addition, NLRP13 protein level of stable THP-1 cells was decreased upon *P.aeruginosa* infection, that signifies NLRP13 cleavage by Casp-8 (Figure 5.9). With Co-IP, we showed that NLRP13 interacts with Casp-8. These results show that NLRP13 might be involved in Casp-8 activation complex.

Along with core components of the inflammasome complex, expression of MALT1 was amplified in stably-NLRP13 expressing THP-1 cells upon *P.aeruginosa* infection. MALT1, which is a paracaspase, is one of the essential regulators of NF-κB activation and NLRP3 inflammasome [35]. We also showed that NLRP13 contributes to phosphorylation of IκB-α upon infection. All of these findings suggest NLRP13 enhances activation of inflammasome complex through NF-κB activation. Interestingly, increasing protein level of NLRP3 upon infection was enhanced by NLRP13 overexpression. From this inspection, it could be speculated that NLRP13 may have a regulatory role on NLRP3-inflammasome. In this scenario, NLRP13 is probably involved in activation of Casp-8 through FADD-Casp-8 complex which in turns activates canonical NLRP3-inflammasome [23].

P.aeruginosa infection significantly increases the NLRP13 expression. The increasing levels of NLRP13 lead to increasing expression of IL-1β and IL-6 as expected and consistent with the results of WB and ELISA. When NLRP13 was knocked-down using CRISPR-Cas9 system, expression of IL-1β was decreased upon *P.aeruginosa* infection. The opposite influences of overexpression and knock-down systems of NLRP13 on expression of IL-1β further demonstrated that NLRP13 activates pro-inflammatory mechanisms to deal with infection of *P.aeruginosa*. If NLRP13 had functions only in assembly of inflammasome complex, we expected knock-down of NLRP13 could not affect the expression of inflammasome components. However, we observed decrease in expression of IL-1β with NLRP13-knock down in response to *P.aeruginosa* showing

that NLRP13 may have a role in activation of transcription factors related with innate immune responses such as NFκB. This finding is consistent with increase in MALT-1 expression by NLRP13 overexpression upon *P.aeruginosa* infection. In addition, we demonstrated that NLRP13 has additive effects on secretion of TNF-α and IL-6 upon both LPS/ATP treatment and *P.aeruginosa* infection. From literature, we know that secretion of TNF-α and IL-6 result from NFκB activation. All of them shows that NLRP13 has a role for NFκB.

NLRP13 increased the population of $CD11b^+$ upon extended PMA-differentiation followed by LPS/ATP treatment. CD11b is common surface marker for macrophages. We expected such a result because Casp-8 has a crucial role in macrophage differentiation. When treated with LPS/ATP, THP-1 macrophages produces a 70 kDa cleaved form of NLRP13 and this cleavage was blocked with pan-caspase inhibitor (Figure 5.19). Besides, NLRP13 is cleaved by Casp-8 giving rise two cleaved product around 40 and 70 kDa that was demonstrated by *in vitro* cleavage assay (Figure 5.23). Collectively, it could be speculated that augmentation of CD11b expression upon LPS/ATP treatment is aroused from cleavage of NLRP13 by Caspase-8. In addition, ERK inhibitors decreases expression of CD11b and blocking of PI3K-AKT pathway leads to decrease in expression of both CD11c and CD80 [36]. Accordingly, NLRP13 may contribute to macrophage differentiation through activation of ERK and PI3K-AKT, since we observed that NLRP13 increases activation of ERK and AKT in PMA-differentiated THP-1 macrophages.

Along with macrophage differentiation, macrophage polarization was investigated. According to our data, NLRP13 increases secretion of IL-1β, TNF-α, IL-6, IL-8, and MIP-1-β, while decreases secretion of IL-10. As NLRP13 shows pro-inflammatory M1 phenotype, we expected NLRP13 leads to increase in expression of M1 marker, CD80. We observed that NLRP13 significantly increased the expression of CD80 upon LPS/ATP treatment as we expected. However, unexpectedly, extended PMA differentiation increased CD163 expression of stably-NLRP13 expressing THP-1 cells. Instead of monocytes-derived human macrophages (MDMs), THP-1 acute monocytic leukemia

cell line is generally preferred for *in vitro* studies due to their limited life span and inter-individual variability. However, malignant background of THP-1 might affect macrophage polarization differently from MDMs. Tedesco S. and colleagues studied whether PMA-differentiated THP-1 cells are reliable alternative for MDMs for examining M1/M2 polarization. They showed secretion pattern for a set of cytokines including IL-1β, TNF-α, ıL-6, and MIP-1-β is same in MDM and PMA-differentiated THP-1, while a set of cytokines like IL-8 shows different patterns. In addition, they observed that M1 polarization gives similar response for CD80 expression in MDM and PMA-differentiated THP-1 and M2 polarization behave unexpected fashion for CD206 and CD163 in PMA-differentiated THP-1 [37]. Despite of unexpected staining of CD163 in stably-NLRP13 expressing THP-1 macrophages, all of the other data indicate NLRP13 influences cells into pro-inflammatory M1-like fashion.

We observed that extended PMA-differentiation increase pro-inflammatory role of NLRP13 upon LPS and ATP treatment, otherwise it cancels positive outcome of NLRP13 against *P.aeruginosa* infection. The negative impact of PMA-differentiation on *P.aeruginosa*-induced secretion of cytokines was considered as whether overexpression of NLRP13 cause the THP-1 monocytes differentiated into dentritic cells instead of macrophages upon *P.aeruginosa* infection. Actually, overexpression of NLRP13 did not improve expression of neither M1/M2 nor cDC/pDC markers. Unexpected finding about CD163 clarifies the negative impact of PMA-differentiation on infection.

Interestingly, stable expression of NLRP13 increased activation of AKT and ERK upon PMA differentiation and LPS/ATP treatment, while it did not affect the phosphorylation of ERK and negatively regulated the phosphorylation of AKT in the case of *P.aeruginosa* infection. As mentioned earlier, PMA directly induces ERK activation. Stable expression of NLRP13 also increased phophorylation of ERK. Additionally, PI3K/Akt regulates survival during macrophages differentiation against differentiation induced apoptotis maintaining NF-κB-dependent expression of anti-apoptotic Bcl-xL [36]. *P.aeruginosa* is a opportunistic gram-negative bacteria which have different secretion systems. With type 3 secretion system, inner rod-proteins

sensed by NLRC4. Besides, pore forming toxins activates NLRP3 inflammasome and *P.aeruginosa* escape intracellular killing bu inducing macrophage autophagy through NLRP3-inflammasome [38]. In case of infection, less activation of AKT in stably-NLRP13 expressing cells might be explained as induction of pyroptotic cell death. In addition, a heteroglycan from the cyanobacterium Nostoc commune decreases LPS induced AKT phosphorylation in THP-1 cells [39]. We do not know which virulent agent of *P.aeruginosa* induce NLRP13, it may have such an effect.

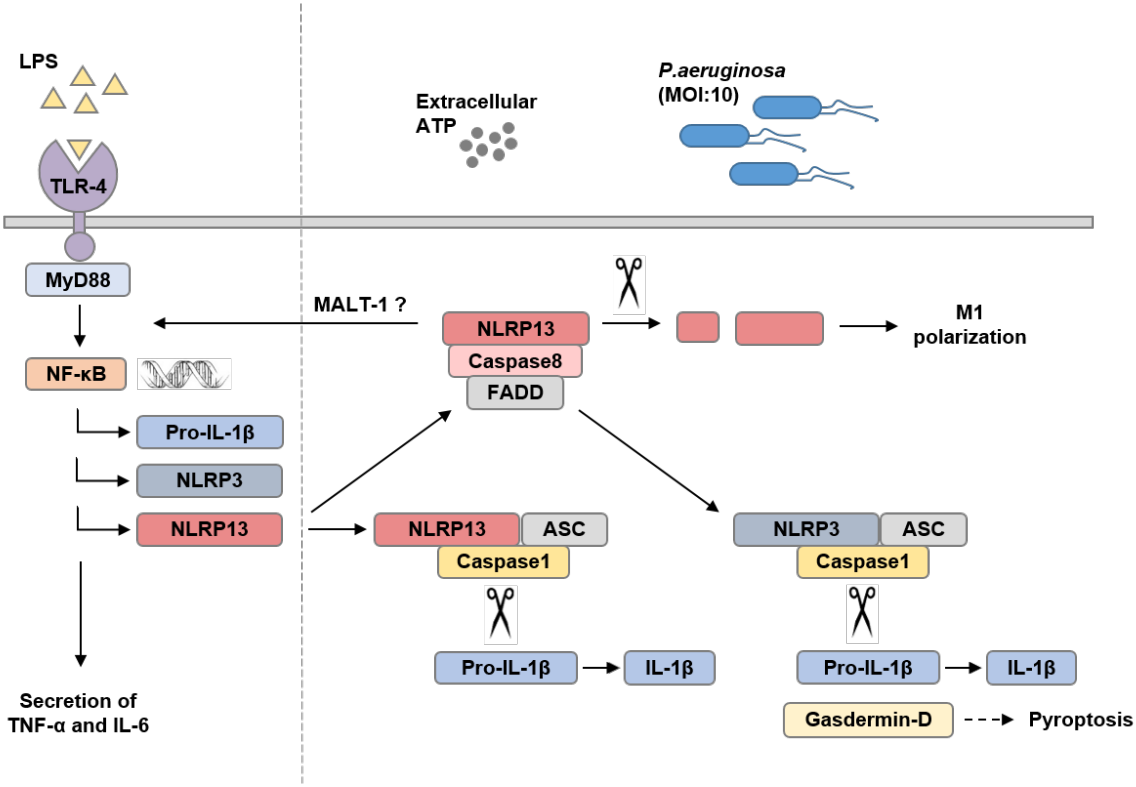

Figure 6.1. Proposed model for NLRP13-driven innate immune responses.

Based upon our results, we propose that NLRP13 inflammasome is activated by LPS/ATP and *P.aeruginosa*. With inclusion of TLR-4 signaling concomitantly to NLR-signaling, NF-κB activation leads to expression of pro-inflammatory molecules including pro-IL-1β, NLRP3, and NLRP13. After activation signal, NLRP13 follows two alternative routes. Firstly, NLRP13 forms inflammasome complex together with ASC and pro-Casp-1 leading to activation of pro-Casp-1 which in turns results in

cleavage of pro-IL-1β and secretion of IL-1β and other pro-inflammatory cytokines like TNF-α and IL-6. Secondly, NLRP13 is included in caspase-8 activating complex. Enhanced activation of Casp-8 leads to increase activity of NLRP3-inflammasome. Post-translational cleavage of NLRP13 by Casp-8 results in differentiation towards to M1 phenotype. In addition, NLRP13 enhances NF-κB activation probably through MALT-1 leading to secretion of TNF-α and IL-6 and engendering a positive feed back loop to deal with *P.aeruginosa* infection. (Figure 6.1)

In order to further clarify our proposed model for NLRP13, the role of NLRP13 in activation of Casp-8 would be studied. Gasdermin-D induced pyroptosis would be affected by NLRP13 either through the NLRP3-inflammasome or its own inflammasome. The effects of NLRP13 on inflammasome activation might be studied in NLRP3-knock out cell lines to see in which routes, from our proposed model, NLRP13 is preferably found.

REFERENCES

1. Takeuchi, O. and S. Akira, "Pattern Recognition Receptors and Inflammation", *Cell*, Vol. 140, No. 6, pp. 805–820, 3 2010.

2. Beutler, B., "Inferences, questions and possibilities in Toll-like receptor signalling", *Nature*, Vol. 430, No. 6996, pp. 257–263, 7 2004.

3. Akira, S., S. Uematsu and O. Takeuchi, "Pathogen Recognition and Innate Immunity", *Cell*, Vol. 124, No. 4, pp. 783–801, 2 2006.

4. Chiffoleau, E., "C-Type Lectin-Like Receptors As Emerging Orchestrators of Sterile Inflammation Represent Potential Therapeutic Targets", *Frontiers in Immunology*, Vol. 9, p. 227, 2 2018.

5. Metzger, R. N., A. B. Krug and K. Eisenächer, "Enteric Virome Sensing-Its Role in Intestinal Homeostasis and Immunity.", *Viruses*, Vol. 10, No. 4, 2018.

6. Kim, Y. K., J. S. Shin and M. H. Nahm, "NOD-Like Receptors in Infection, Immunity, and Diseases.", *Yonsei medical journal*, Vol. 57, No. 1, pp. 5–14, 1 2016.

7. Kobayashi, K., N. Inohara, L. D. Hernandez, J. E. Galán, G. Núñez, C. A. Janeway, R. Medzhitov and R. A. Flavell, "RICK/Rip2/CARDIAK mediates signalling for receptors of the innate and adaptive immune systems", *Nature*, Vol. 416, No. 6877, pp. 194–199, 3 2002.

8. Murdoch, S., U. Djuric, B. Mazhar, M. Seoud, R. Khan, R. Kuick, R. Bagga, R. Kircheisen, A. Ao, B. Ratti, S. Hanash, G. A. Rouleau and R. Slim, "Mutations in NALP7 cause recurrent hydatidiform moles and reproductive wastage in humans", *Nature Genetics*, Vol. 38, No. 3, pp. 300–302, 3 2006.

9. Can Sahillioglu, A., F. Sumbul, N. Ozoren and T. Haliloglu, "Article Structural

and Dynamics Aspects of ASC Speck Assembly", *Structure/Folding and Design*, Vol. 22, pp. 1722–1734, 2014.

10. Lamkanfi, M. and V. M. Dixit, "Leading Edge Review Mechanisms and Functions of Inflammasomes", *Cell*, Vol. 157, pp. 1013–1022, 2014.

11. Latz, E., T. S. Xiao and A. Stutz, "Activation and regulation of the inflammasomes", *Nat Rev Immunol*, Vol. 13, No. 6, 2013.

12. Kousathana, F., M. Georgitsi, V. Lambadiari, E. J. Giamarellos-Bourboulis, G. Dimitriadis and M. Mouktaroudi, "Defective production of interleukin-1 beta in patients with type 2 diabetes mellitus: Restoration by proper glycemic control", *Cytokine*, Vol. 90, pp. 177–184, 2 2017.

13. Jin, T., A. Perry, J. Jiang and et al., "Structures of the HIN domain:DNA complexes reveal ligand binding and activation mechanisms of the AIM2 inflammasome and IFI16 receptor.", *Immunity*, Vol. 36, No. 4, pp. 561–71, 4 2012.

14. Chavarría-Smith, J. and R. E. Vance, "Direct Proteolytic Cleavage of NLRP1B Is Necessary and Sufficient for Inflammasome Activation by Anthrax Lethal Factor", *PLoS Pathogens*, Vol. 9, No. 6, p. e1003452, 6 2013.

15. Miao, E. A., D. P. Mao, N. Yudkovsky, R. Bonneau, C. G. Lorang, S. E. Warren, I. A. Leaf and A. Aderem, "Innate immune detection of the type III secretion apparatus through the NLRC4 inflammasome.", *Proceedings of the National Academy of Sciences of the United States of America*, Vol. 107, No. 7, pp. 3076–80, 2 2010.

16. Qu, Y., S. Misaghi, A. Izrael-Tomasevic, K. Newton, L. L. Gilmour, M. Lamkanfi, S. Louie, N. Kayagaki, J. Liu, L. Kömüves, J. E. Cupp, D. Arnott, D. Monack and V. M. Dixit, "Phosphorylation of NLRC4 is critical for inflammasome activation", *Nature*, Vol. 490, No. 7421, pp. 539–542, 8 2012.

17. Bauernfeind, F. G., G. Horvath, A. Stutz, E. S. Alnemri, K. MacDonald, D. Speert,

T. Fernandes-Alnemri, J. Wu, B. G. Monks, K. A. Fitzgerald, V. Hornung and E. Latz, "Cutting edge: NF-kappaB activating pattern recognition and cytokine receptors license NLRP3 inflammasome activation by regulating NLRP3 expression.", *Journal of immunology (Baltimore, Md. : 1950)*, Vol. 183, No. 2, pp. 787–91, 7 2009.

18. Bartlett, R., L. Stokes and R. Sluyter, "The P2X7 receptor channel: recent developments and the use of P2X7 antagonists in models of disease.", *Pharmacological reviews*, Vol. 66, No. 3, pp. 638–75, 7 2014.

19. Py, B. F., M.-S. Kim, H. Vakifahmetoglu-Norberg and J. Yuan, "Deubiquitination of NLRP3 by BRCC3 critically regulates inflammasome activity.", *Molecular cell*, Vol. 49, No. 2, pp. 331–8, 1 2013.

20. Rathinam, V. A. K., S. K. Vanaja, L. Waggoner, A. Sokolovska, C. Becker, L. M. Stuart, J. M. Leong and K. A. Fitzgerald, "TRIF licenses caspase-11-dependent NLRP3 inflammasome activation by gram-negative bacteria.", *Cell*, Vol. 150, No. 3, pp. 606–19, 8 2012.

21. Yang, D., Y. He, R. Muñoz-Planillo, Q. Liu and G. Núñez, "Caspase-11 requires the pannexin-1 channel and the purinergic P2X7 pore to mediate pyroptosis and endotoxic shock", .

22. Gringhuis, S. I., T. M. Kaptein, B. A. Wevers, B. Theelen, M. van der Vlist, T. Boekhout and T. B. H. Geijtenbeek, "Dectin-1 is an extracellular pathogen sensor for the induction and processing of IL-1β via a noncanonical caspase-8 inflammasome", *Nature Immunology*, Vol. 13, No. 3, pp. 246–254, 3 2012.

23. Gurung, P., P. K. Anand, R. K. S. Malireddi, L. Vande Walle, N. Van Opdenbosch, C. P. Dillon, R. Weinlich, D. R. Green, M. Lamkanfi and T.-D. Kanneganti, "FADD and caspase-8 mediate priming and activation of the canonical and noncanonical Nlrp3 inflammasomes.", *Journal of immunology (Baltimore, Md. : 1950)*, Vol. 192,

No. 4, pp. 1835–46, 2 2014.

24. Kayagaki, N., I. B. Stowe, B. L. Lee, K. O'Rourke, K. Anderson, S. Warming, T. Cuellar, B. Haley, M. Roose-Girma, Q. T. Phung, P. S. Liu, J. R. Lill, H. Li, J. Wu, S. Kummerfeld, J. Zhang, W. P. Lee, S. J. Snipas, G. S. Salvesen, L. X. Morris, L. Fitzgerald, Y. Zhang, E. M. Bertram, C. C. Goodnow and V. M. Dixit, "Caspase-11 cleaves gasdermin D for non-canonical inflammasome signalling", *Nature*, Vol. 526, No. 7575, pp. 666–671, 10 2015.

25. Liu, X., Z. Zhang, J. Ruan, Y. Pan, V. G. Magupalli, H. Wu and J. Lieberman, "Inflammasome-activated gasdermin D causes pyroptosis by forming membrane pores.", *Nature*, Vol. 535, No. 7610, pp. 153–8, 2016.

26. Chu, J.-Q., G. Shi, Y.-M. Fan, I.-W. Choi, G.-H. Cha, Y. Zhou, Y.-H. Lee and J.-H. Quan, "Production of IL-1β and Inflammasome with Up-Regulated Expressions of NOD-Like Receptor Related Genes in Toxoplasma gondii-Infected THP-1 Macrophages", *The Korean Journal of Parasitology*, Vol. 54, No. 6, pp. 711–717, 12 2016.

27. Han, J., Y. Jun, S. H. Kim, H.-H. Hoang, Y. Jung, S. Kim, J. Kim, R. H. Austin, S. Lee and S. Park, "Rapid emergence and mechanisms of resistance by U87 glioblastoma cells to doxorubicin in an in vitro tumor microfluidic ecology", *Proceedings of the National Academy of Sciences*, Vol. 113, No. 50, pp. 14283–14288, 12 2016.

28. Gültekin, Y., *Cloning and Characterization of Novel Nod Like Receptors as Cytoplasmic Immune Sensors*, Ph.D. Thesis, Bogazici University, 2011.

29. Mustafa Yalçınkaya, *Characterization of NLRP13 in Inflammasome Activity*, Ph.D. Thesis, Bogazici University, 2015.

30. Mundle, S. D., P. Venugopal, J. D. Cartlidge, D. V. Pandav, L. Broady-Robinson,

S. Gezer, E. L. Robin, S. R. Rifkin, M. Klein, D. E. Alston, B. M. Hernandez, D. Rosi, S. Alvi, V. T. Shetty, S. A. Gregory and A. Raza, "Indication of an involvement of interleukin-1 beta converting enzyme-like protease in intramedullary apoptotic cell death in the bone marrow of patients with myelodysplastic syndromes.", *Blood*, Vol. 88, No. 7, pp. 2640–7, 10 1996.

31. Wallach Erika Gustafsson, D., P. Ramakrishnan, T. Jurewicz, A. Waisman, O. Brenner, R. Haffner, Y. Pewzner-Jung, N. Yogev, A. Tae-Bong Kang and T. Ben-Moshe, "Nonapoptotic Roles Caspase-8 Serves Both Apoptotic and", *J Immunol References*, Vol. 173, pp. 2976–2984, 2018.

32. Martinez, F. O. and S. Gordon, "The M1 and M2 paradigm of macrophage activation: time for reassessment.", *F1000prime reports*, Vol. 6, p. 13, 2014.

33. Mendoza, M. C., E. E. Er and J. Blenis, "The Ras-ERK and PI3K-mTOR pathways: cross-talk and compensation.", *Trends in biochemical sciences*, Vol. 36, No. 6, pp. 320–8, 6 2011.

34. Hoffmann, J. C., A. Pappa, P. H. Krammer and I. N. Lavrik, "A new C-terminal cleavage product of procaspase-8, p30, defines an alternative pathway of procaspase-8 activation.", *Molecular and cellular biology*, Vol. 29, No. 16, pp. 4431–40, 8 2009.

35. Liu, W., W. Guo, N. Hang, Y. Yang, X. Wu, Y. Shen, J. Cao, Y. Sun and Q. Xu, "MALT1 inhibitors prevent the development of DSS-induced experimental colitis in mice via inhibiting NF-κB and NLRP3 inflammasome activation.", *Oncotarget*, Vol. 7, No. 21, pp. 30536–49, 5 2016.

36. Busca, A., M. Saxena, S. Iqbal, J. Angel and A. Kumar, "PI3K/Akt regulates survival during differentiation of human macrophages by maintaining NF-κB-dependent expression of antiapoptotic Bcl-xL", *Journal of Leukocyte Biology*, Vol. 96, No. 6, pp. 1011–1022, 12 2014.

37. Tedesco, S., F. De Majo, J. Kim, A. Trenti, L. Trevisi, G. P. Fadini, C. Bolego, P. W. Zandstra, A. Cignarella and L. Vitiello, "Convenience versus Biological Significance: Are PMA-Differentiated THP-1 Cells a Reliable Substitute for Blood-Derived Macrophages When Studying in Vitro Polarization?", *Frontiers in pharmacology*, Vol. 9, p. 71, 2018.

38. Deng, Q., Y. Wang, Y. Zhang, M. Li, D. Li, X. Huang, Y. Wu, J. Pu and M. Wu, "Pseudomonas aeruginosa Triggers Macrophage Autophagy To Escape Intracellular Killing by Activation of the NLRP3 Inflammasome.", *Infection and immunity*, Vol. 84, No. 1, pp. 56–66, 1 2016.

39. Olafsdottir, A., G. E. Thorlacius, S. Omarsdottir, E. S. Olafsdottir, A. Vikingsson, J. Freysdottir and I. Hardardottir, "A heteroglycan from the cyanobacterium Nostoc commune modulates LPS-induced inflammatory cytokine secretion by THP-1 monocytes through phosphorylation of ERK1/2 and Akt", *Phytomedicine*, Vol. 21, No. 11, pp. 1451–1457, 9 2014.

APPENDIX A: PLASMID MAPS

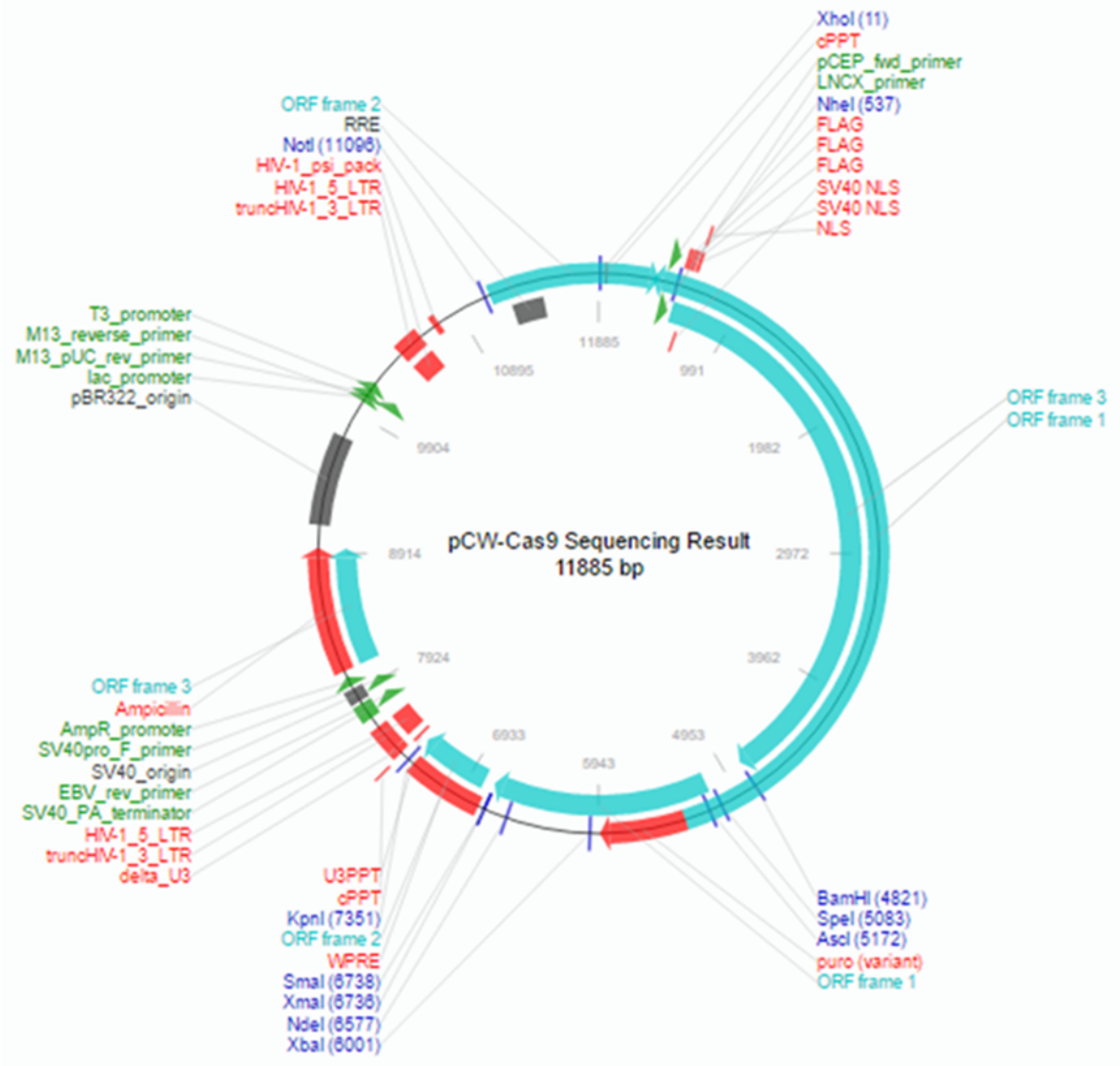

Figure A.1. Map of the pCW-Cas9 vector.

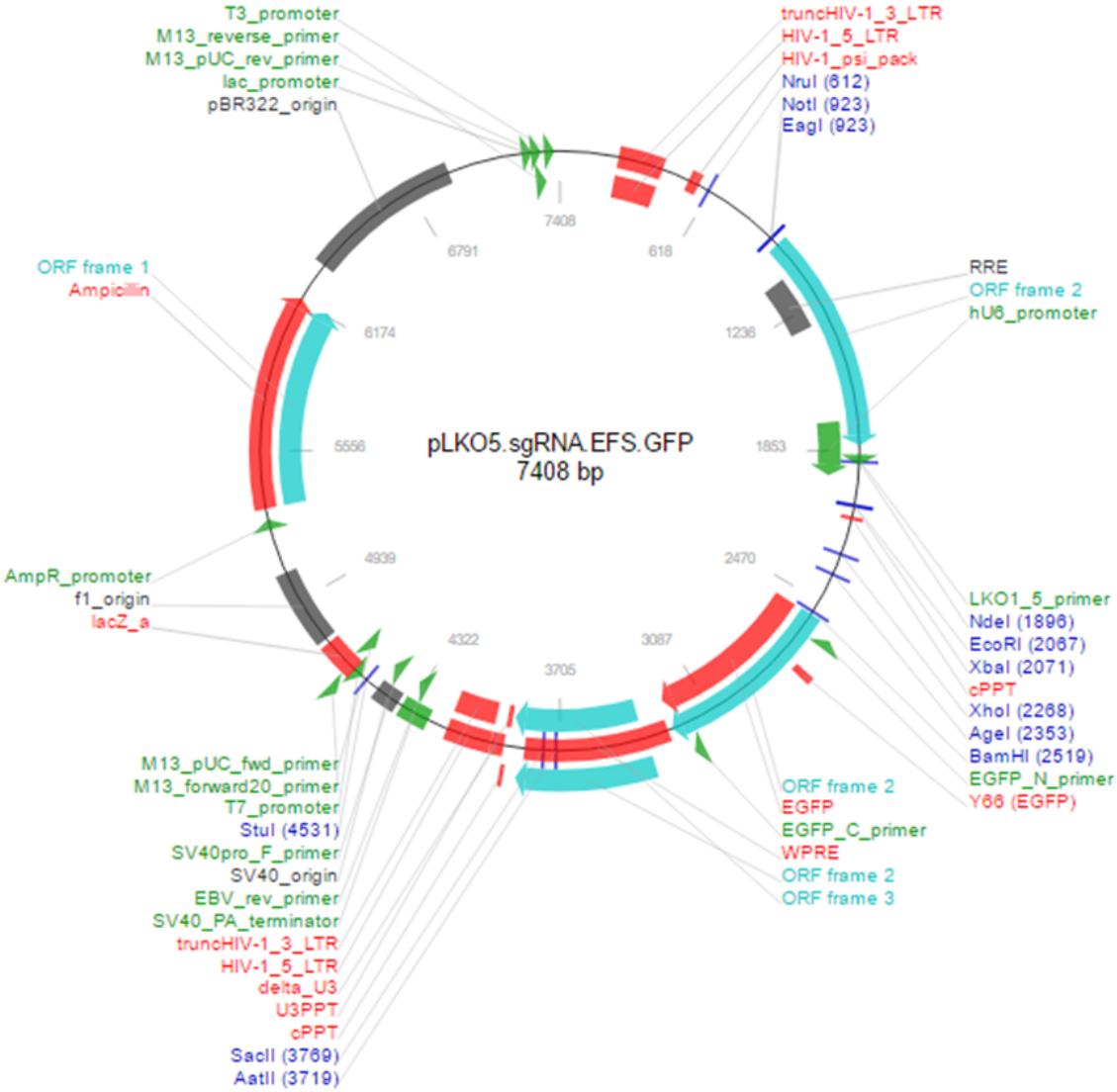

Figure A.2. Map of the pLKO5.sgRNA.EFS.GFP vector.